

ORIGINAL ARTICLE

Large and interacting effects of temperature and nutrient addition on stratified microbial ecosystems in a small, replicated, and liquid-dominated Winogradsky column approach

Marcel Suleiman  | Yves Choffat | Uriah Daugaard | Owen L. Petchey

Department of Evolutionary Biology and Environmental Studies, University of Zurich, Zurich, Switzerland

Correspondence

Marcel Suleiman, Department of Evolutionary Biology and Environmental Studies, University of Zurich, Zurich, Switzerland.
Email: marcel.suleiman@ieu.uzh.ch

Funding information

Forschungskredit of the UZH, Grant/Award Number: FK-20-125; Swiss National Science Foundation, Grant/Award Number: Project 310030_188431

Abstract

Aquatic ecosystems are often stratified, with cyanobacteria in oxic layers and phototrophic sulfur bacteria in anoxic zones. Changes in stratification caused by the global environmental change are an ongoing concern. Increasing understanding of how such aerobic and anaerobic microbial communities, and associated abiotic conditions, respond to multifarious environmental changes is an important endeavor in microbial ecology. Insights can come from observational and experimental studies of naturally occurring stratified aquatic ecosystems, theoretical models of ecological processes, and experimental studies of replicated microbial communities in the laboratory. Here, we demonstrate a laboratory-based approach with small, replicated, and liquid-dominated Winogradsky columns, with distinct oxic/anoxic strata in a highly replicable manner. Our objective was to apply simultaneous global change scenarios (temperature, nutrient addition) on this micro-ecosystem to report how the microbial communities (full-length 16S rRNA gene seq.) and the abiotic conditions (O_2 , H_2S , TOC) of the oxic/anoxic layer responded to these environmental changes. The composition of the strongly stratified microbial communities was greatly affected by temperature and by the interaction of temperature and nutrient addition, demonstrating the need of investigating global change treatments simultaneously. Especially phototrophic sulfur bacteria dominated the water column at higher temperatures and may indicate the presence of alternative stable states. We show that the establishment of such a micro-ecosystem has the potential to test global change scenarios in stratified eutrophic limnic systems.

KEYWORDS

anaerobes, cyanobacteria, global change, oxygen, phototrophic sulfur bacteria

This is an open access article under the terms of the Creative Commons Attribution-NonCommercial-NoDerivs License, which permits use and distribution in any medium, provided the original work is properly cited, the use is non-commercial and no modifications or adaptations are made.

© 2021 The Authors. *MicrobiologyOpen* published by John Wiley & Sons Ltd.

1 | INTRODUCTION

Micro-organisms are key players in nearly all ecosystems, ranging from the human gut to marine and freshwater habitats. The functioning of microbial communities is critical for many ecosystem services since micro-organisms are the driving force behind biogeochemical cycles (Falkowski et al., 2008; Kertesz, 2000; Stein & Klotz, 2016; Weiss et al., 2003). Nevertheless, microbes are highly dependent on environmental conditions; even slight changes can lead to taxonomic and functional community shifts (Allison et al., 2013; Evans & Wallenstein, 2014). Consequently, microbial communities and their functions are significantly affected by global change (Cavicchioli et al., 2019), which has recently led to the emergence of the research field termed “Global Change Microbiology” (Boetius, 2019).

Stratification of lakes is a common seasonal phenomenon of the temperate zone, which is dependent on the depth and the surface area of the lake (Gorham & Boyce, 1989). Stratified lakes show warm and oxygen-rich upper water layers, dominated by cyanobacteria and algae, and colder (anoxic) deeper layers, that harbor heterotrophic biomass-degraders and sulfate-reducing bacteria (Diao et al., 2017, 2018; Guggenheim et al., 2020; Vigneron et al., 2021). In between these layers, the metalimnion can be found, which is formed by decreasing light-intensities and oxygen concentrations (microaerophilic), and an increasing pool of reduced sulfur compounds, creating ideal niches for phototrophic sulfur bacteria and chemolithoautotrophic micro-organisms (Bush et al., 2017; Diao et al., 2017, 2018; Jorgensen et al., 1979; Morrison et al., 2017; Nyirabuhoro et al., 2020; Savvichev et al., 2018; Vavourakis et al., 2019; Vigneron et al., 2021; Wörner & Pester, 2019; Wu et al., 2019).

Besides chemical and physical parameters that influence the presence of oxic and anoxic layers, it was recently postulated that mutual inhibition between cyanobacteria and anaerobic sulfur-dependent bacteria creates and maintains the distinct oxic and anoxic zones of such ecosystems (Bush et al., 2017). The mathematical model used in that study predicts abrupt transitions between aerobic and anaerobic microorganisms and the occurrence of oxic–anoxic regime shifts. Moreover, studies have demonstrated that global change consequences could have strong impacts on this sensitive ecosystem, including dominant growth of harmful cyanobacteria due to warming (Posch et al., 2012), or increasing primary production and creation of anoxic layers due to increased nutrient input (Luek et al., 2017).

The mentioned studies show that important insights come from analyses of observations of naturally occurring aquatic ecosystems (Vigneron et al., 2021), and theoretical models of the plausible and relevant ecological and biochemical processes. In addition, in the field of global change biology, targeted experiments that employ a limited number of standardized synthetic model ecosystems have been described as an “entirely different approach” (Hutchins et al., 2019) and are considered vital alongside studies of naturally occurring ecosystems (Lahti et al., 2014) and hybrids of both approaches (De Vos et al., 2017). Key challenges in global change microbiology that are amenable to research with synthetic ecosystems include the role of evolutionary processes, the role of historical contingency

(Widder et al., 2016) and interactions among micro-organisms (Overmann & van Gemerden, 2000), and the integration of data and theory (Widder et al., 2016). Experiments about the role of environmental, organismal interactions, and biochemical feedbacks in stratified aquatic micro-ecosystems appear absent, however.

Establishing a suitable such standardized model ecosystem for analyzing potential responses of a broad range of micro-organisms remains crucial. Being able to monitor global change responses of diverse functional groups of potentially interacting microbes is a desirable feature of such an experimental system, which points toward systems with strong abiotic gradients in space and or time. In this work, we get inspiration from an “old” but highly valuable approach, the Winogradsky column (Dworkin, 2012; Pagaling et al., 2017; Zavarzin, 2006). We constructed a modified and smaller version that allows a highly replicable development of a broad range of complex and dynamic microbial groups in one experimental unit. In contrast to classical Winogradsky columns, our micro-ecosystems are mostly liquid, with only a small sediment layer (~6% v/v of the column). Thus, we created a highly replicable liquid oxic–anoxic interphase and self-developing model systems.

By applying this approach, we were able to analyze microbial responses to multifarious environmental change (temperature and nutrient addition manipulated factorially), including the responses of community composition and abiotic environmental conditions. As well as showing how microbial community composition, dissolved oxygen, pH, and hydrogen sulfide respond to temperature and nutrient addition, we highlight the potential for global change microbiology research of this new approach coupled with state-of-the-art sequencing technologies.

We hypothesize that higher temperature will increase the dominance of anaerobic microbes due to an increase in the extent of the anoxic zone, due to the lower solubility of oxygen in warmer water. We hypothesize that nutrient addition (addition of ammonium phosphate, highly used fertilizer (Cao et al., 2018)) will alter community composition, but we cannot a priori say how, as this would depend on features of the organisms, such as competitive and facilitative interactions among them, which we do not have sufficient information about. We did not have any a priori expectation of whether the combined effect of temperature and nutrient addition would be additive (no interaction), more than additive (positive interaction), or less than additive (negative interaction). We anticipated the potential for micro-ecosystems to become entirely oxic or entirely anoxic, and for changes in composition to be non-linear and to potentially include discontinuous responses that are predicted by theory.

2 | MATERIALS AND METHODS

2.1 | Preparation of micro-ecosystems

The vessels used to house the micro-ecosystems were standard glass test tubes (diameter 13 mm, height 16 cm). Each was equipped with two oxygen sensors (PreSens Precision Sensing GmbH), one at a height of 4 cm (bottom sensor) and the other at 14 cm (top sensor), both stuck

to the inside surface of the test-tube wall. These sensors allow optical measurements of oxygen to be taken through the wall of a test tube.

Each test tube (which we also refer to as a “column”) had a butyl rubber stopper on top, with two cannulas. The longer cannula (StericanR, length 120 mm, diameter 0.8 mm) reached the depth of the bottom O₂ sensor and was covered with an oxygen-protecting plug (BD Plug). The shorter cannula (length 40 mm, 0.9 mm diameter) was always open and extended only into the headspace of the micro-ecosystem. This shorter cannula, therefore, allowed for gas exchange between the headspace and the atmosphere (Figure 1a).

Micro-ecosystems were established from sediment and water samples were taken in July from a small pond in Zürich, Switzerland (47°23'51.2"N 8°32'33.3"E, the temperature of 24.6°C, pH of 6.7) at a depth of 30 cm. In total, 200 g of sediment and 2 L water were collected. The sediment sample was supplemented with sterile 0.5% crystalline cellulose, 0.5% methyl-cellulose, 1% CaSO₄, 0.2% CaCO₃, and 0.01% NH₄H₂PO₄. Sediment was homogenized by mixing for 30 min before each test tube was filled with sediment up to a height of 1.5 cm (in 0.5 cm steps, with constant mixing of the source sediment bottle between steps). Sediment that stuck to the inner wall of the test tube was removed carefully in all cases. Columns were filled with well-homogenized 16 ml pond water (supplemented with 0.01% NH₄H₂PO₄), leaving approximately 1 cm of headspace. In contrast to classical Winogradsky columns (Dworkin, 2012; Rundell et al., 2014; Zavarzin, 2006), our set-up is dominated by liquid and contains a small amount of sediment. Columns were incubated at room temperature for two hours without light to allow the sediment to settle fully, after

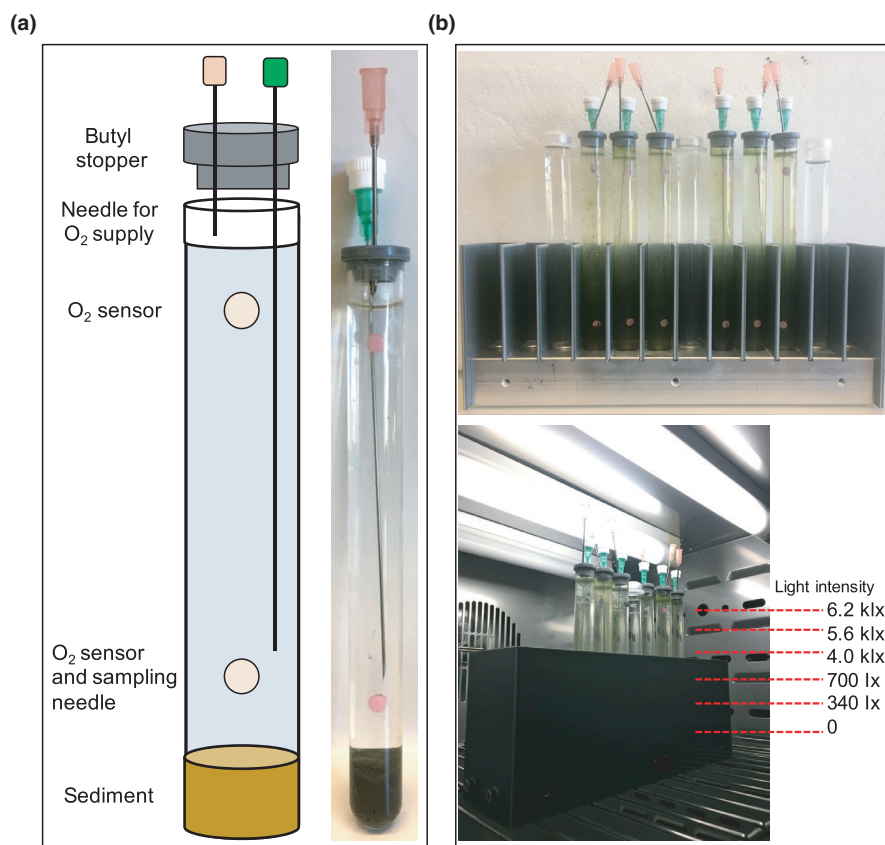
which an initial oxygen concentration of the top and the bottom sensor was recorded and the columns were placed in incubators.

2.2 | Incubation and treatments

Each column was incubated at one of seven temperatures: 12, 16, 20, 24, 28, 32, or 36°C. Incubators (Pol Eco Apparatura sp.j.) were equipped with two fluorescent light sources (PHILIPS Master TL8W/840) with a dark-light cycle of 8:16 hours. Columns were placed in a 1.5-cm hole in a metal base so that the sediment layer was continuously kept in darkness. Up to a height of 10 cm, the columns were surrounded by a plastic holder that causes a gradient of light, ranging from 340 lx at the intersphere of sediment:water at the bottom and up to 700 lx at the top of the light-protector (Figure 1b). The top of the column experienced the fluorescent light intensity of 6200 lx. Each holder contained six columns, in two groups of three replicates, separated by a water-filled column. This arrangement was placed in the middle of both light sources in the incubator, allowing the same light intensity at the back and front of each column.

A second treatment was the manipulation of nutrient concentration. For this, 0.1% NH₄H₂PO₄ was added to half of the columns by taking 16 µl of a sterile 10% NH₄H₂PO₄ solution, while 16 µl sterile water was used for the controls. This treatment was performed once per week (day 1, 8, 14, 20) and was factorially crossed with the temperature treatment, resulting in 7 (temperature) × 2 (nutrient levels) and 3 replicated, giving a total of 42 columns. These were incubated for 22 days.

FIGURE 1 Preparation and incubation conditions of the micro-ecosystems. (a) Columns were filled with 1.5 cm sediment and pond water with supplementary resources (see main text for details). Columns were equipped with two oxygen sensors (top and bottom) and closed with a butyl rubber stopper. One cannula allows gas exchange between the headspace and the atmosphere (pink). A second cannula is used for taking samples at the bottom sensor (green, anoxic stopper). (b) Micro-ecosystems were incubated in light-gradient-producing holders. Sediment was covered inside the metal base (1.5 cm depth) for incubation without light. Columns were, thereby, incubated with a light gradient ranging from 6.2 kilolux (klx) to 0 lux (lx)



2.3 | Sampling and measurements

Liquid samples were taken on days 8, 14, and 20 by collecting 200 μ l of liquid from the bottom of the columns by using the installed canula. This liquid was used to measure H_2S (Microsensor, AMT Analysenmesstechnik GmbH) and was replaced with anoxic sterile lake water. Non-invasive oxygen measurements were performed at the top and bottom sensor of the columns (every day except for days 5, 11, 12, and 17). Oxygen concentration is presented in percentage, saturation adjusted for the prevailing temperature and pressure (e.g., 21% saturation occurs when water is in equilibrium with the surrounding atmosphere). Thus, the known effect of temperature on oxygen solubility does not affect our analyses.

After incubation, all columns were destructively sampled. For each column, the whole water column (16 ml) and the sediment layer were processed separately. One replicate of each treatment combination had the water column separated at the height of the bottom oxygen layer, giving a sample of the upper and lower liquid layer, as well as a sample, for the sediment. Each sample was centrifuged (16,000 rpm, 3 min) and pellets were frozen at $-80^{\circ}C$ until DNA extraction. The supernatant was used for pH measurements, as well as total nitrogen and total organic carbon analysis. While sampling, the H_2S concentration at the sediment-water interphase was measured under anoxic conditions.

2.4 | DNA extraction, 16S rRNA gene amplification

DNA extractions were performed with ZymoBIOMICS DNA Microprep Kit (ZymoResearch), following the manufacturer's instructions. 16S rRNA gene amplifications were performed with 27F forward primer (5'-AGRGTTYGATYMTGGCTCAG-3') and 1592R reverse primer (5'-RGYTACCTTGTTACGACTT-3'), resulting in an amplification product of \sim 1500 bp. Primers were equipped with 5'phosphate and a 5'buffer sequence of GCATC. Barcodes, PCR chemicals, and conditions (27 cycles) were performed as suggested by Pacific Biosciences (PacBio, 2020). PCR products were visualized on a 1% (w/v) agarose gel and were pooled with equal concentrations. Afterward, PCR products were purified using AMPure[®]PB beads (PacBio), following the manufacturer's guidelines. Besides 16S rRNA gene amplification for PacBio long-read sequencing, also DGGE analysis performed as described previously (Antranikian et al., 2017; Suleiman et al., 2019) to identify the white bacterial population.

2.5 | Library preparation and sequencing

Sequencing was performed at the Functional Genomic Center Zürich, Switzerland. The SMRT bell was produced using the SMRTbell Express Template Prep Kit 2.0 (PacBio). The input amplicon pool concentration was measured using a Qubit Fluorometer dsDNA High Sensitivity assay (Life Technologies). A Bioanalyzer 12 Kb assay (Agilent) was used to assess the amplicon pool size distribution. 0.75 μ g of amplicon pool was DNA damage repaired

and end-repaired using polishing enzymes. Ligation was performed to create the SMRT bell template, according to the manufacturer's instructions. The SMRT bell library was quality inspected and quantified using a Bioanalyzer 12 Kb assay (Agilent) and on a Qubit Fluorimeter (Life technologies), respectively. A ready-to sequence SMRT bell-Polymerase Complex was created using the Sequel II Binding Kit 2.1 and Internal Control 1.0 (PacBio) according to the manufacturer's instruction. The Pacific Biosciences Sequel II instrument was programmed to sequence the library on 1 Sequel II SMRT Cell 8 M, taking 1 movie of 15 h per cell, using the Sequel II Sequencing Kit 2.0 (PacBio). Sequencing data quality was checked, via the PacBio SMRT Link software, using the "run QC module".

2.6 | Bioinformatics

Bioinformatics was performed using R and the package Dada2 (Callahan et al., 2016). In short, reads were filtered regarding primer sequences, length (1300–1600 bp), quality, error rates, and chimeras. The outcome of the filter processes can be observed for each sample (Appendix Table A1). Finally, the constructed sequence table was aligned with the SILVA ribosomal RNA database (Quast et al., 2012), using version 138 (non-redundant dataset 99). Afterward, a phyloseq formatted data object was constructed, containing the amplicon sequence variant (ASV) table, taxonomy table, and sample metadata, using the package phyloseq (McMurdie & Holmes, 2013), which was also used for microbial community analysis together with the vegan package (Oksanen et al., 2019). All sequences that were assigned to "chloroplast" were removed from the phyloseq file since primers were chosen for bacterial 16S rRNA gene and bind incorrectly to chloroplast sequences.

Microbial community composition was analyzed with non-metric multidimensional scaling (NMDS), using the metaMDS function from the vegan package. NMDS was used because a principal component analysis of the compositional variation exhibited a strong "arch-effect", which can hinder the use of ordination scores in further analyses that we wanted to make. The metaMDS function was instructed to use Bray-Curtis distance, to transform the data to have 2-dimensions. The metaMDS function was instructed to try 200 different starting positions to assure convergence. NDMS was performed on relative abundances of sequences with a relative abundance of at least 1% in at least one sample. The 2-dimensional NDMS solution converged with a stress of 0.15. A 3-D solution converged with a stress of 0.11. This suggests that the 2-D solution is a good representation of the compositional variation among the samples and that the 3-D solution is not much better. Linear models with appropriate error structures were used to assess the weight of evidence supporting causal effects of treatments and treatment interactions on response variables. All analyses involving NDMS and variables derived from it were repeated with a different standardization (centered log ratios) and a different distance measure (Aitchison distance) (Gloor et al., 2017). These different methods did not affect the conclusion of the strong and relatively linear effect of

temperature on composition (NMDS1) and a non-linear and interacting effect of temperature and nutrient treatment on composition (NMDS2).

We intentionally avoid referring to effects as significant or not significant, and rather use the terms: no evidence $p > 0.1$, weak evidence $0.1 > p > 0.05$, moderately strong evidence $0.05 > p > 0.01$, strong evidence $0.01 > p > 0.001$, very strong evidence $p < 0.001$.

3 | RESULTS

3.1 | Macroscopic observations

All columns developed a stratified growth of colorful micro-organisms within the incubation time, regardless of the temperature and nutrient-addition treatment (Figure 2a,b). Macroscopical and microscopical observation of morphology and color indicated that the micro-ecosystems likely consisted of a relatively large upper layer of cyanobacteria and algae and phototrophic sulfur bacteria in a smaller lower layer. Moreover, a white layer occurred in all columns during the first 10 days

(Figure 2c) at different positions depending on the incubation temperature (12°C and 16°C below the bottom sensor, and at higher temperatures above the bottom sensor). DGGE analysis identified this layer as a community of species of the microaerophilic genus *Magnetospirillum*, indicating that this layer is the oxic–anoxic interphase of the micro-ecosystems. In general, all micro-ecosystems developed an oxic and anoxic part (Figure 5), and triplicates of each treatment combination predominantly showed comparable growth and development. The gas formation was observed in the sediment layers of the columns, indicating an active microbial community (Figure 2d).

3.2 | Relative abundances of microbial taxa of the water column

To study the microbial communities in detail, full-length 16S rRNA gene sequencing was performed. Removal of sequences that did not occur at more than 1% in at least one sample resulted in 343 different amplicon sequence variants (from initial 5633 unique sequences in all samples).

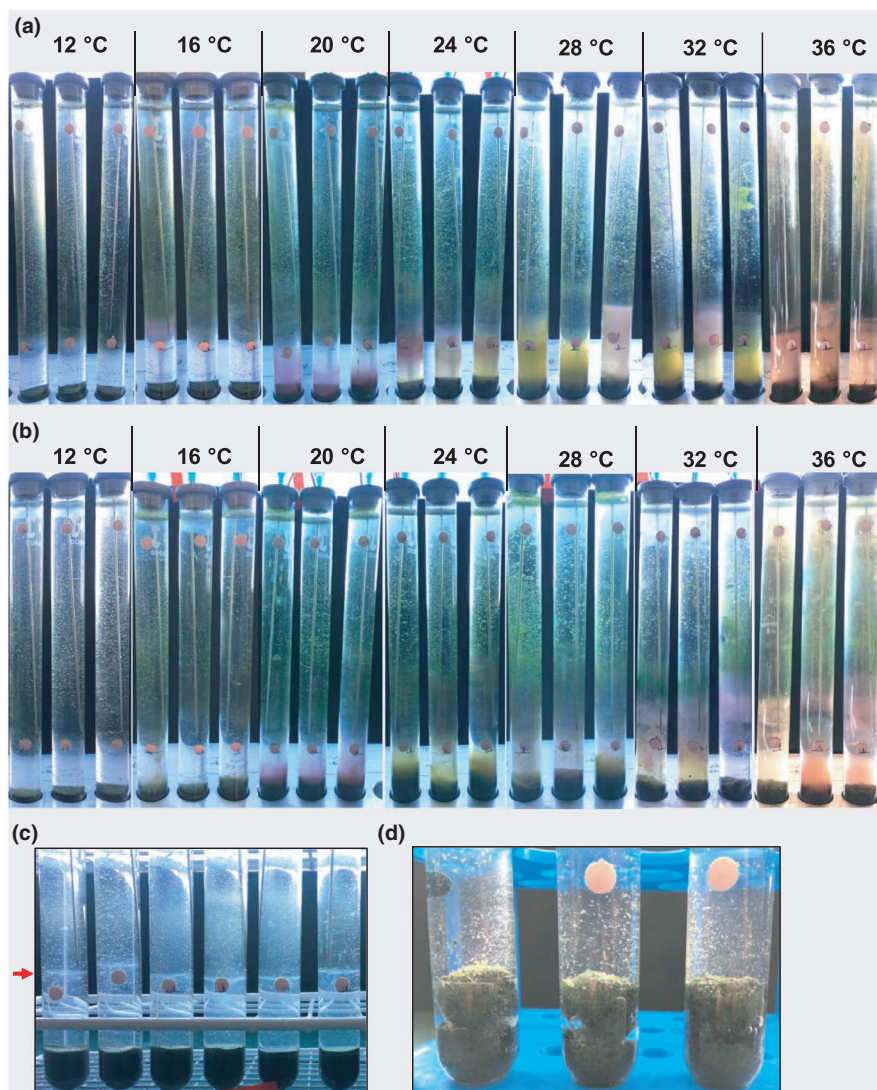


FIGURE 2 Macroscopical observation of the micro-ecosystems. (a) Control micro-ecosystems (triplicates) after incubation at 12–36°C for 22 days. (b) Nutrient-addition micro-ecosystems (triplicates) after incubation at 12–36°C for 22 days. (c) Observation of a white bacterial cloud within 10 days of incubation. Exemplary columns incubated at 20°C of day 10 are shown. The red arrow highlights the position of the cloud. (d) Gas formation in the sediment layers, exemplary picture taken at day 12 of columns incubated at 28°C

All of the micro-ecosystems at 12°C were dominated by members of the order *Burkholderiales* (54–69%) (Figure 3a, Appendix Figure A1 for details). Relative abundance of *Burkholderiales* decreased to 15–37% (control) and 29–53% (nutrient addition) at 16°C, and relative abundance of *Rhodospirillales* increased up to 23%. At 20°C, members of *Chlorobiales* and *Chromatiales* became more abundant. Members of *Chlorobiales* were dominant in all micro-ecosystems at 24°C (33–64% controls, 62–64% nutrient-addition treatments), 28°C (42–92% controls, 35–70% nutrient-addition treatments), and 32°C (78–90% controls, 18–50% nutrient addition). At 36°C, members of *Chlorobiales* disappeared, and in no-nutrient-addition treatments, members of the cyanobacterial order *Limnitrachales* were dominant (up to 25%; but none occurred in nutrient-addition treatment).

The full-length 16S rRNA amplicon gene sequencing resulted in a detailed account of the microbial community to the genus level (Figure 3b, Appendix Figures A2–A8 for details). All micro-ecosystems at 12°C (Figure 3b, Appendix Figure A2) were dominated by members of the aerobic genus *Giesbergia* (controls 22–34%, nutrient addition 57–67%), followed by *Aquaspirillum* in the controls and *Flavobacterium* in the nutrient-addition micro-ecosystems. At 16°C (Figure 3b, Appendix Figure A3), control micro-ecosystems were dominated by members of the aerobic genus *Uliginosibacterium* (12–27%), which had a very low relative abundance in the nutrient-addition treatment (less than 2%). In contrast, *Giesbergia* and *Aquaspirillum* (4–35%) were very abundant in the nutrient-addition treatment.

Genus composition at 20°C (Figure 3b, Appendix Figure A4) included anaerobic phototrophic sulfur bacteria, in particular the green sulfur bacteria *Chlorobium* appeared highly abundant in the nutrient-addition treatments (up to 46%) and the purple sulfur bacteria *Chromatium* in all micro-ecosystems at this temperature (up to 28%). With increasing temperature, green sulfur bacteria *Chlorobium*, and *Chlorobaculum* genera increased in relative abundance. At 24°C (Figure 3b, Appendix Figure A5), *Chlorobium* and *Chlorobaculum* were detected in the controls, with 11–39% and 6–25% relative abundance, respectively, and in the nutrient-addition treatments with 39–65% and 27–60%. Furthermore, the picocyanobacterial genus *Cyanobium* appeared (up to 7%) in the control micro-ecosystems.

At 28°C (Figure 3b, Appendix Figure A6), green sulfur bacteria continued to increase their dominance, especially *Chlorobium* (up to 92%). Interestingly, the *Control_3* column consisted of a comparable lower amount of green sulfur bacteria, but additionally of the purple sulfur bacteria *Allochromatium* (41%). This finding can be confirmed by the macroscopical observation of the pink layer (Figure 3a). Additionally, the *Nutrient addition_2* column consisted of *Chlorobaculum* instead of *Chlorobium* in contrast to the *Nutrient addition_1* and *Nutrient addition_3* columns.

At 32°C (Figure 3b, Appendix Figure A7), *Chlorobium* dominated the control-micro-ecosystems, while this genus also had lower though still high relative abundance in the nutrient-addition treatments (up to 52%).

At 36°C (Figure 3b, Appendix Figure A8), the microbial community changed again: *Chlorobium* and *Chlorobaculum* disappeared totally. Present instead were the facultatively anaerobic, sulfur-oxidizing bacterium *Sulfuricurvum* (up to 49%), the cyanobacterial genera *Nostoc* (up to 36%), and *Limnothrix* (up to 25%), and the phototrophic sulfur bacteria *Phaeospirillum* (up to 11%).

Separate sequencing and analysis of the upper and lower layer of liquid revealed a dominance of phototrophic sulfur bacteria in the lower anoxic layer and of cyanobacteria in the upper oxic layer of the columns (Appendix Figure A9).

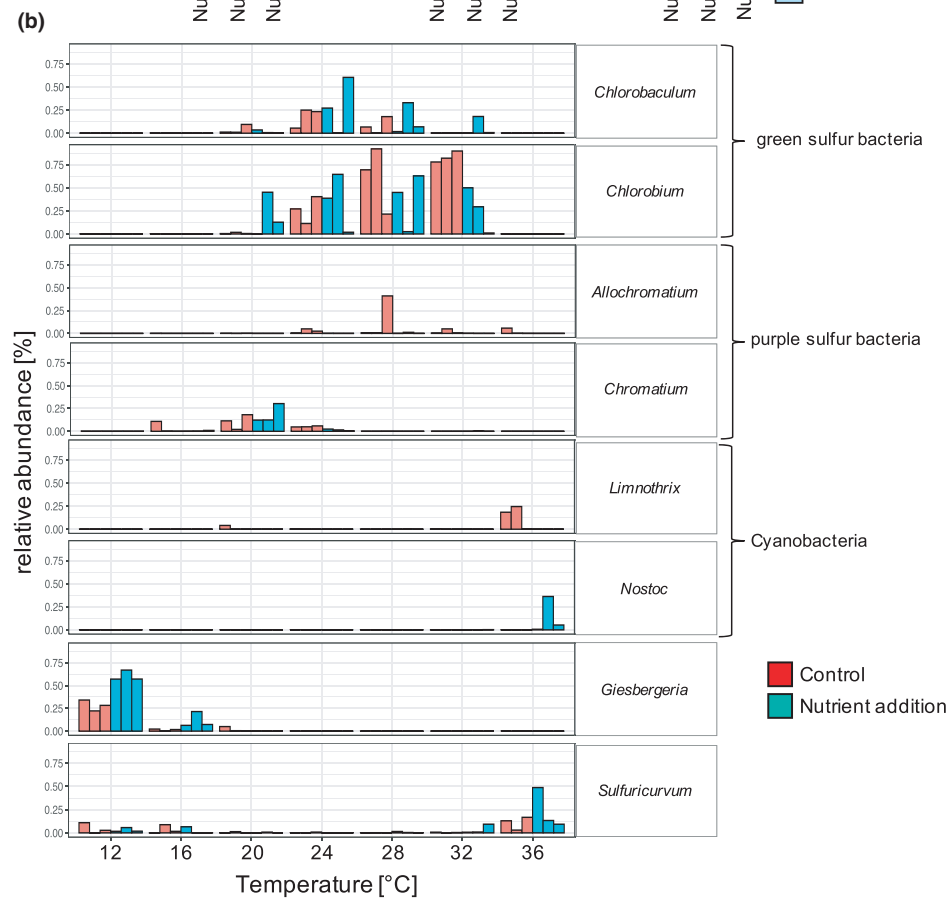
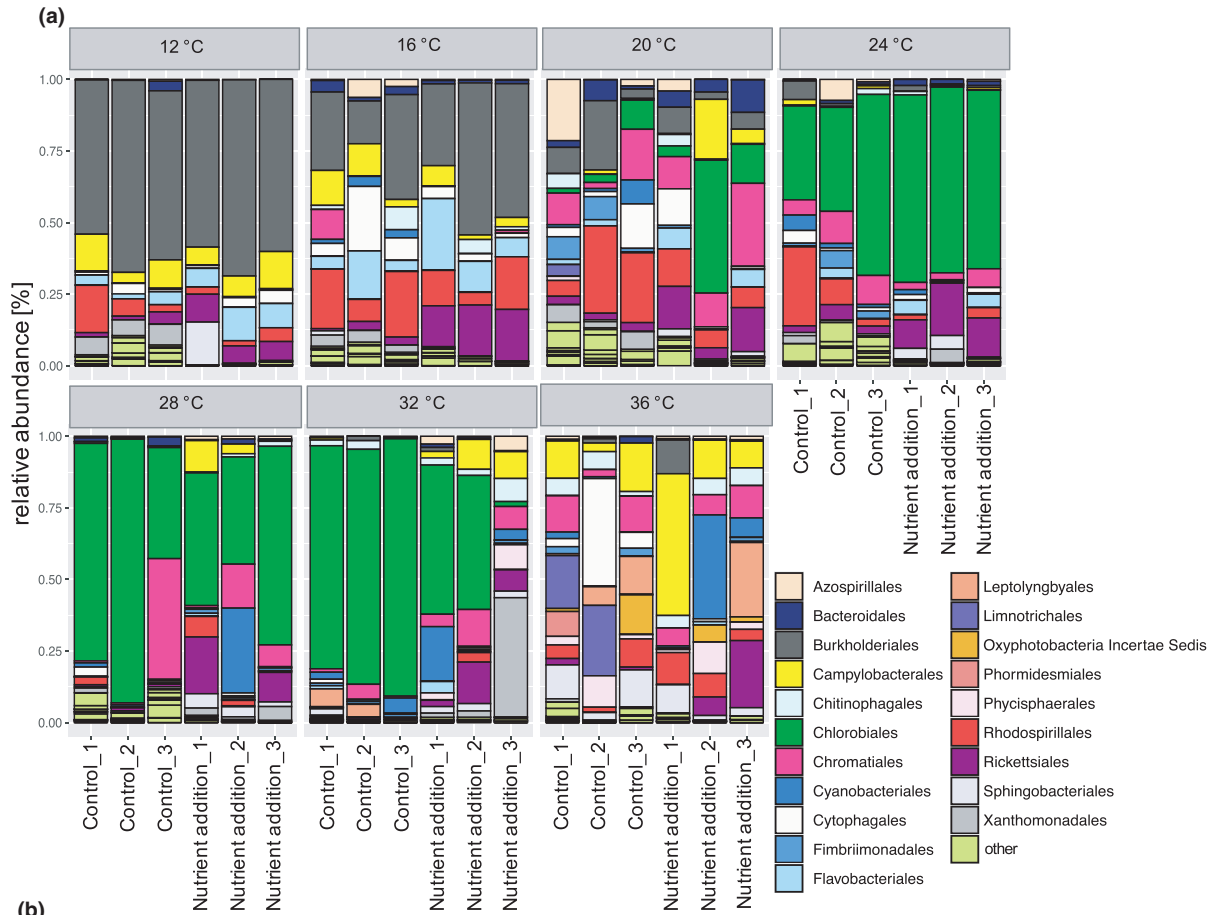
3.3 | Community composition (NMDS) of the water column

The effects of temperature and nutrient addition on the relative abundance described in the previous sections were very evident in the analyses of community composition via NMDS (Figure 4a). Compositional variation along the first NMDS axis (hereafter NMDS1) was strongly associated with temperature, but not with the nutrient-addition treatment, nor the interaction of the temperature and nutrient-addition treatment (Figure 4b; Table 1). In contrast, compositional variation along NMDS2 was affected by a strong interaction between temperature and the nutrient-addition treatment (Figure 4c; Table 1). Effects of temperature on NMDS2 scores were non-linear in both the control and the nutrient-addition treatments. In the control treatment, the NMDS2 score remained constant from 12 to 24°C and then decreased up to 36°C. In contrast, in the nutrient-addition treatment, NMDS2 values first decrease (12 to 16°C), then increase (16 to 28/32°C), and then decrease again (32 to 36°C).

3.4 | Microbial communities within the sediments

The community composition of taxonomic orders in the sediment was comparable to that in the water column (Appendix Figure A10), though a high relative abundance of *Chlorobiales* and *Chromatiales* was detected between 20 and 32°C. All ecosystems (except 12°C) were rich in the relative abundance of members of the anaerobic order *Spirochaetales* (up to 48%). On the genus level, however, the community consisted of a majority of sequences that could not be assigned to known taxonomic groups. With a focus on sulfate-reducing micro-organisms, the

FIGURE 3 Microbial community composition of the micro-ecosystems. (a) Relative abundance on order level is shown for each micro-ecosystem. Orders with relative abundances <7% in all samples were assigned to “other.” (b) Relative abundance of 8 dominant and functional important genera depending on the temperature and treatment conditions. Red bars represent control triplicates, blue bars nutrient-addition triplicates



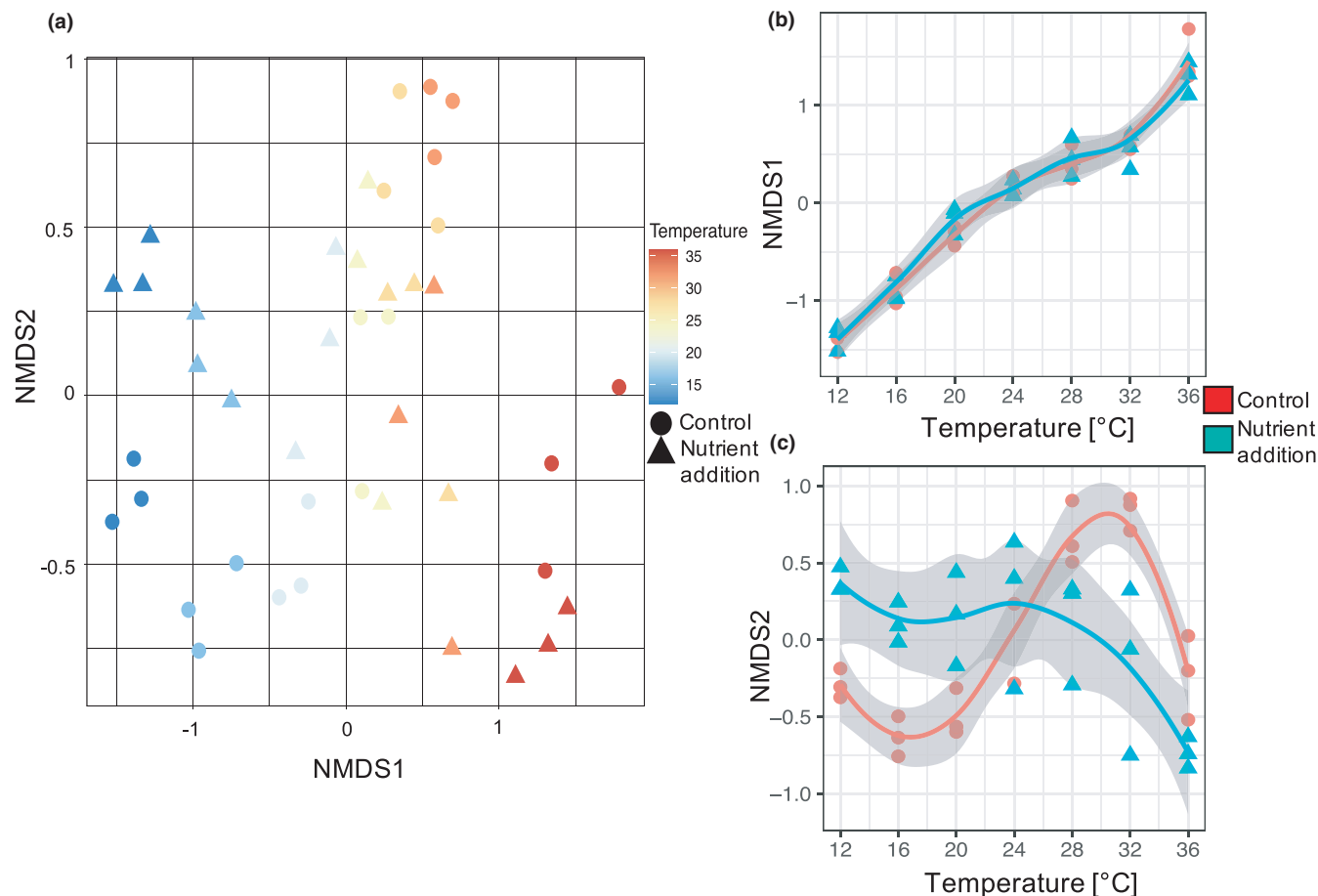


FIGURE 4 Variation in microbial community composition. (a) NMDS scores based on Bray–Curtis distance showing the variation in microbial community composition of the water column (b) The effect of temperature and nutrient addition on NMDS1. (c) The effect of temperature and nutrient addition on NMDS2. (b,c) Control micro-ecosystems are shown as red circles, nutrient addition-treated micro-ecosystems as blue triangles. Lines are local polynomial regressions; gray ribbons show the 95% confidence intervals

sediment-harbored members of the order *Desulfotomaculales* up to 2%. Besides that, genera including *Desulfobulbus*, *Desulfovibrio*, *Desulfovirga*, *Desulfomicrobium*, *Desulforhabdus*, were detected, but all in a low relative abundance of less than 1%. Furthermore, members of the anaerobic biomass-degrading family *Clostridiaceae* made up to 5% of the communities, depending on the temperature.

3.5 | Oxygen dynamics

Oxygen concentration in the top of the columns increased within the first 10 days in all incubations and then remained oxic until the end of the experiment (Figure 5a). Moreover, oxygen concentrations in the upper part of the columns were in general higher than 21% (concentration expected if in equilibrium with the atmosphere) and sometimes reached up to 60%. We assume that oxygen production took place at the upper part of the columns by the algae and cyanobacteria, causing this high level of dissolved oxygen. The controls and the nutrient addition-treated columns showed only slight differences in their oxygen levels.

The long-term effect of temperature and nutrient addition on oxygen concentration in the upper part of the columns was calculated as the mean of the oxygen concentration during the last three days of the experiment (Figure 5c). There was very strong evidence that temperature decreased the oxygen concentration from about 35% at 12°C to about 29% at 36°C (Table 1). There was moderately strong evidence that the nutrient-addition treatment reduced oxygen concentration by about 4% irrespective of temperature (i.e., there was no evidence of an interaction; Table 1).

The dynamics of the oxygen concentration of the bottom part of the micro-ecosystems were very different and were strongly affected by temperature and nutrient addition (Figure 5b). At 12°C, a hump-shaped dynamic can be observed, going from anoxic to oxic and back to anoxic during the experiment. The same trend can be observed at 16°C and 20°C, but took place earlier in the experiment. At 24–36°C there was no hump, and conditions were almost entirely anoxic, though with some rapid anoxic-oxic shifts at 16°C, 20°C, 24°C, 28°C, and 36°C at the end of the experiment. These rapid shifts between oxic and anoxic states correspond with shifts in the position of the white microbial population from above (anoxic) to below (oxic) the bottom oxygen sensor (Figure 2c).

TABLE 1 Statistical analysis of the various response variables used in this study. Estimates of the temperature treatment are in units of the response variable per degree Celcius, and estimates of the nutrient-addition treatment are the effect of nutrient addition on the response variable. The interaction estimate is the effect of the nutrient addition on the estimate of the temperature effect. Terms in the main text used for *p*-values: no evidence $p > 0.1$, weak evidence $0.1 > p > 0.05$, moderately strong evidence $0.05 > p > 0.01$, strong evidence $0.01 > p > 0.001$, very strong evidence $p < 0.001$. All models were a general linear model with *F*-tests, except for the bottom oxygen analysis, which was a generalized linear model with binary response variable with likelihood ratio tests (LR-test). The total nitrogen response variable was arcsine square-root transformed before analysis

	Temperature	Nutrient addition	Interaction
Response variable			
Oxygen top			
Estimate	-0.28	-4.32	0.08
Standard error	0.10	3.66	0.14
<i>F</i> -test <i>p</i> -value	1.9e-03	0.05	0.58
Oxygen bottom			
Estimate	-0.23	-3.2	0.23
Standard error	0.12	2.64	0.13
<i>F</i> -test <i>p</i> -value	0.17	0.05	0.05
H ₂ S at sediment-water interphase			
Estimate	-0.17	-12.56	0.43
Standard error	8.59	0.25	0.35
<i>F</i> -test <i>p</i> -value	0.43	0.71	0.21
pH top			
Estimate	-4e-03	3.01	-6e-04
Standard error	9.1e-03	0.33	0.01
<i>F</i> -test <i>p</i> -value	0.49	<2e-16	0.97
pH bottom			
Estimate	0.04	-0.78	-0.03
Standard error	0.01	0.36	0.01
LR-test <i>p</i> -value	2.6e-03	7.27e-15	0.07
Total nitrogen (TN)			
Estimate	-7.8e-04	0.70	-2.7e-03
Standard error	1.7e-03	0.06	2.3e-03
<i>F</i> -test <i>p</i> -value	0.08	<2e-16	0.26

(Continues)

TABLE 1 (Continued)

	Temperature	Nutrient addition	Interaction
Total organic carbon (TOC)			
Estimate	-0.2	12.43	-0.02
Standard error	0.45	15.63	0.63
<i>F</i> -test <i>p</i> -value	0.52	0.02	0.98
NMDS1			
Estimate	0.11	0.22	-0.00825
Standard error	0.005749	0.21	0.008130
<i>F</i> -test <i>p</i> -value	<2e-16	0.99	0.30
NMDS2			
Estimate	0.04	1.77	-0.07
Standard error	0.01	0.41	0.02
<i>F</i> -test <i>p</i> -value	0.85	0.87	6.49e-05

The long-term effect of temperature and nutrient addition on the oxygen concentration of the bottom part of the columns was assessed by transforming the measured oxygen concentration into a binary variable: oxic (O₂ concentration >2%) or anoxic (O₂ concentration <2%). There was moderate evidence of an interaction between temperature and nutrient addition in determining oxic or anoxic state (Table 1). The anoxic state became more likely as temperature increased in the control treatment, but the temperature did not have such an effect in the nutrient-addition treatment (Table 1).

3.6 | Chemical parameters

THE highest H₂S concentrations at the height of the bottom oxygen sensor were measured at 32°C on day 8 (max 6 mg/L) and day 14 (max 5 mg/L), before the H₂S concentration decreased strongly by day 20 (Figure 6a). H₂S on day 22 at the sediment-water interphase was detectable in most micro-ecosystems (Figure 6b), with frequently high concentrations with more than 15 mg/L. However, there was no evidence for an effect of temperature, nutrient addition, or their interaction on H₂S at the end of the experiment (Table 1).

There was very strong evidence that nutrient addition affected the top (Figure 6c) and bottom pH (Figure 6d, Table 1), and additionally strong evidence that temperature affected the bottom pH value. Moreover, the pH of the top and bottom parts of the micro-ecosystems showed clear differences (compare Figure 6c,d). While the control micro-ecosystems had a pH gradient from ~pH 7.5 at the bottom to ~pH 9 at the top, no such gradients occurred in the nutrient-addition treatment, which exhibited a pH of ~6 in both the top and bottom parts of the columns.

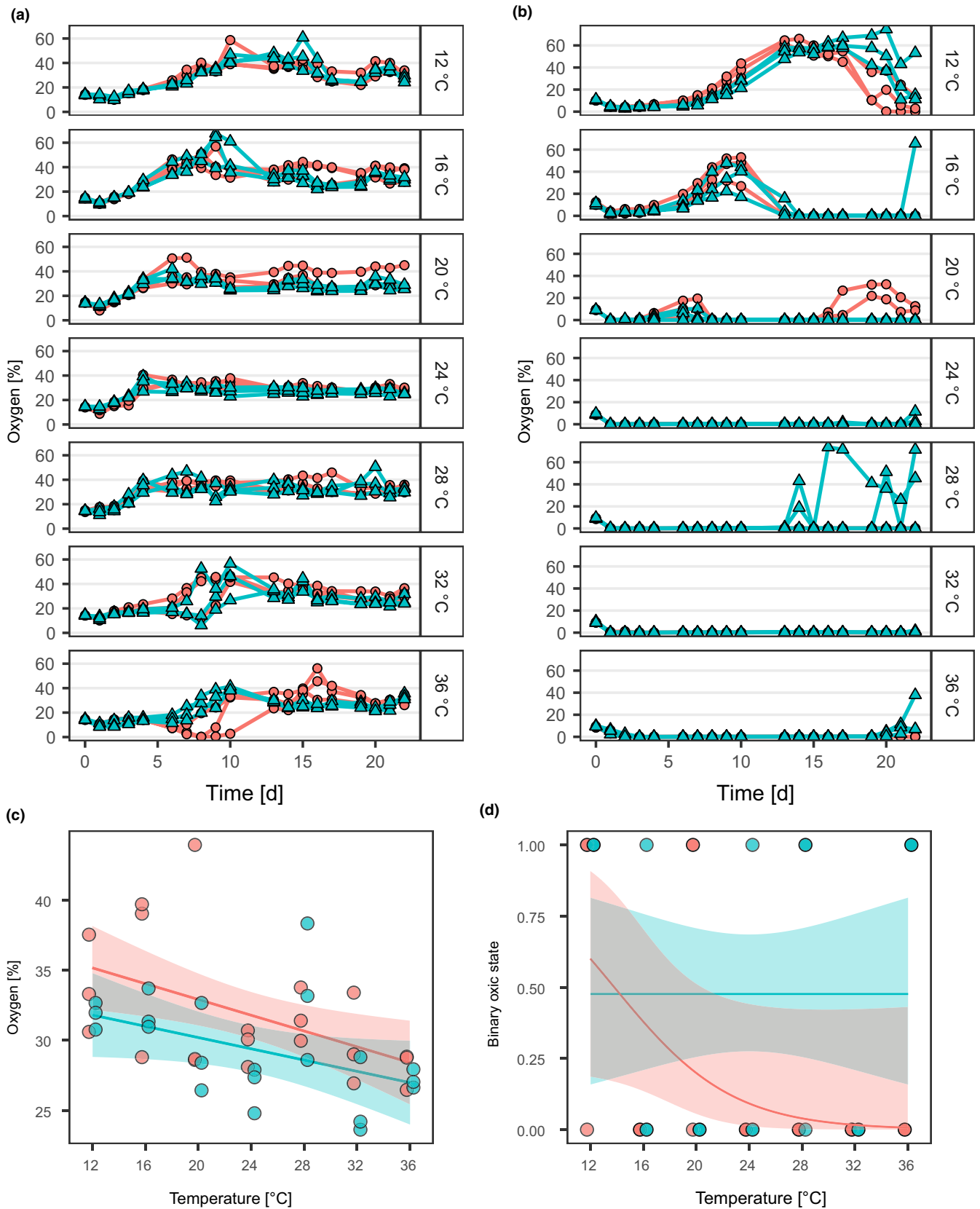


FIGURE 5 Oxygen non-linear dynamics and long-term oxygen-states of the micro-ecosystems. In all panels, control incubations are shown in red circles, nutrient-addition treatments in blue triangles. The oxygen concentration [%] of the micro-ecosystems incubated at different temperatures was measured at the top (a) and bottom (b) sensors over time. (c) The mean of the oxygen concentrations of the top sensor during the last three days of the experiment; lines represent the linear model fit and colored ribbons the 95% confidence intervals. (d) The binary oxygen state at the bottom sensor; lines represent the regression line of the used model and colored ribbons the 95% confidence intervals

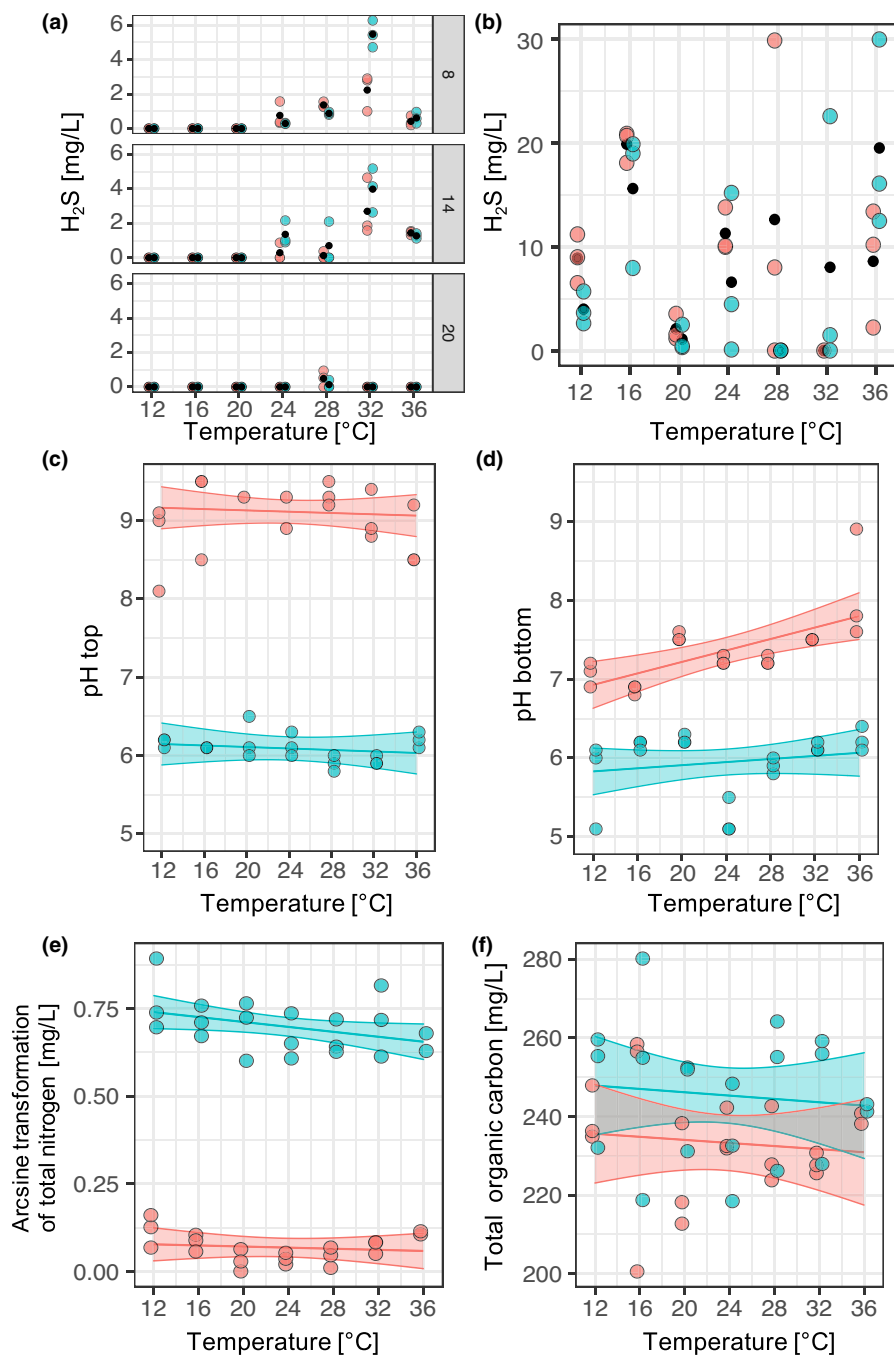


FIGURE 6 Chemical parameters of the micro-ecosystems. (a) Measurement of the Net-H₂S concentration [mg/L] at the bottom oxygen sensor per temperature at incubation days 8, 14, and 20. (b) Measurement of the Net-H₂S concentration [mg/L] at the soil-water interphase per temperature at final incubation day 22. (c) pH of the columns per temperature at the upper part. (d) pH of the columns per temperature at the bottom part. (e) Total nitrogen [mg/L] concentration [mg/L] of the micro-ecosystems depending on incubation temperature. Data were arcsine transformed for statistical analysis. (f) Total organic carbon concentration [mg/L] of the micro-ecosystems depending on incubation temperature. Controls are shown in red dots, nutrient-addition treatments with blue dots. Small black points indicate mean values. Fitted models and confidence intervals (95%) are shown as lines and shaded areas, respectively, for plots for which there was evidence of their significance

Also, total nitrogen (TN) and total organic carbon (TOC) were analyzed for the water column of the micro-ecosystems (Figure 6e,f), and data indicated very strong evidence that nutrient addition increased TN concentration and strong evidence for increasing the TOC concentration (Table 1).

4 | DISCUSSION

Understanding and predicting the consequences of multifarious environmental change is very important in a broad range of research disciplines, and investigations should be made from

global- to micro-scales (Balsler et al., 2006). In contrast to existing work on higher-developed organisms (González-Varo et al., 2013; Pennekamp et al., 2018; Tylianakis et al., 2008), less is known about how bacterial ecosystems react to multifarious global change scenarios (Cavicchioli et al., 2019; Coyle et al., 2017; Hutchins & Fu, 2017; Rillig et al., 2019). Besides, there is a need for experimental studies (in addition to natural systems and mathematical models) of complex microbial model ecosystems that can potentially display diverse responses to changing environmental conditions for various microbial groups in one experimental unit. With inspiration from Winogradsky columns (Dworkin & Gutnick, 2012; Pagaling et al., 2017), we introduce a modified experimental micro-ecosystem, that includes the development of aerobic and anaerobic microbial communities in one experimental ecosystem in a replicable manner. In this study, we demonstrate that such an approach represents an appropriate model system for analyzing responses of complex and stratified microbial communities to global change scenarios.

Some of our results, for example, the stratification and temperature effects, may be considered unsurprising and “textbook knowledge.” This is good evidence that these small and liquid-dominated microbial ecosystems are appropriate analogs of naturally occurring communities. Furthermore, we used this model system to shed light on the consequences of multifarious environmental change, namely simultaneous warming and nutrient deposition—a relatively novel area of ecology, evolution, and microbiology. We hypothesized a simultaneous effect on oxygen dynamics and microbial community compositions. While temperature is considered to be the main driver for shaping soil/sediment communities (Cole et al., 2013; Deng et al., 2018; Garcia-Pichel et al., 2013), we furthermore observed non-additive effects of warming and nutrient addition on the aquatic microbial community (Figure 4c, Table 1). This highlights the importance of studying potential interactions of multiple environmental change parameters simultaneously (Niiranen et al., 2013), given that they can differ in effect compared to the sum of individual disturbances. Environmental change cannot be reduced to the sum of individual factors. It is multifarious, providing the opportunity for “risk multiplication” and for greater challenges when attempting to understand and predict ecosystem responses to environmental change (Schulte to Bühne et al., 2020).

Besides the effect on overall microbial community composition, our results additionally indicated that multiple drivers affect the oxic and anoxic layers differently. The oxic layer of the system was affected by temperature and nutrient addition additively (Figure 5a,c, Table 1). In contrast, the anoxic layers were affected by non-additive effects of temperature and nutrient addition (Figure 5b,c). These observations might be due to the different biogeochemistry processes in the two strata, such as the interplay of specific microbial communities, and their interplay with available nutrients, trace elements, as well as abiotic factors, and the presence of specific oxygen-reducing sulfur compounds (Bush et al., 2017; Chapra & Canale, 1991; Garcia et al., 2013; Jorgensen et al., 1979; Luther et al., 2003; Yu et al., 2014).

The microbial community composition and the oxygen dynamics are tightly coupled in a feedback loop. Key players in this feedback loop are oxygen-producing cyanobacteria, sulfate-reducing bacteria, and phototrophic sulfur bacteria (Bush et al., 2017; Lee et al., 2014). While cyanobacteria and especially green and purple sulfur bacteria had high relative abundance in the micro-ecosystems, the relative abundance of sulfate-reducing micro-organisms was comparably low. This observation could be explained by the sampling schedule: detection of high H_2S concentration within the micro-ecosystems indicates a nutrient-rich habitat for phototrophic sulfur bacteria (Guerrero et al., 1985; Hamilton et al., 2014), which suggests the previous high activity of sulfate-reducing micro-organisms (Pimenov et al., 2014; Sass et al., 1997). Earlier or later sampling may have revealed more oxidized sulfur compounds and a higher abundance of sulfate-reducing micro-organisms. Further explanation of this unbalanced ratio between these two functional groups could probably be found in the light-dark- and the sediment-water ratio of our model system. With increasing temperature, micro-organisms changed from aerobic representatives (*Giesbergeria*, *Uliginosibacterium*) to anaerobic ones (*Chlorobaculum*, *Chlorobium*), which is also confirmed by the oxygen measurements. The higher turnover rate of organic substrates of the microbes in the sediment and higher H_2S production supports the dominant growth of phototrophic sulfur bacteria at moderate and higher temperatures (Findlay & Kamyschny, 2017; Nedwell et al., 1994; Velthuis et al., 2018). The dominant blooms of *Chlorobium* with increasing temperature is an important finding and its ecological consequences should be investigated for future global change scenarios.

Some results hint at the presence of alternate stable states (Beisner & Cuddington, 2010) in the phototrophic sulfur bacterial communities. There was considerable variation among some of the replicates of the same treatment combination, despite them having very similar initial conditions. For example, some contained either the green phototrophs *Chlorobium* or *Chlorobaculum*, or the purple phototroph *Allochromatium* (based on sequencing and macro/microscopical observation of the respective columns). Besides these alternative compositions within the same functional group, also the oxygen dynamics indicated interesting patterns, particularly at 28°C, where two of three replicates of the nutrient addition-treated micro-ecosystems became oxic at the bottom sensor. Since no significant differences in the microbial community can be observed in these incubations, vertical movements of the oxic-anoxic interphase may have occurred, which was also visible by the different heights of the white microbial community, consisting of *Rhodospirillaceae* representatives. Additionally, the sinking of cyanobacteria into the anoxic layer could also result in temporary changes in oxygen dynamics in our dynamic system.

An interesting aspect could be observed regarding the pH gradient of the water column, which showed a slightly alkaline pH on the water surface in the controls, probably due to photosynthesis reactions of cyanobacteria/algae and HCO_3^- in the unbuffered system, and a slightly acidic pH at the bottom, probably due to organic matter degradation. This gradient was removed by the addition of

$\text{NH}_4\text{H}_2\text{PO}_4$, which decreases the pH due to its acidic character and buffering activity on the surface to pH ~6.

5 | CONCLUSION

This study reveals that two environmental change factors (i.e., temperature and nutrient availability) caused large and non-additive variation in the composition of aquatic microbial communities and the abiotic conditions of the ecosystem. The advantages of this system include high parallelization and replication, easy and non-destructive sampling, the versatility of testable conditions and manipulations, and are of additional interest besides in situ ecosystem studies. We believe that these insights are only the tip of the iceberg of what can be learned from such a model micro-ecosystems with strong and even stratified spatial environmental gradients. Even in the described study, we could have included many more elements, such as characterization of the conditions at the sampling site, measurements of organic compounds composition in the water column, and control without cellulose. Further research with this new experimental system could take many paths, including studying the stability of the communities to press and pulse perturbations, and how this stability may depend on aspects of community composition, such as functional composition and intraspecific diversity; the extent and significance of evolutionary processes such as mutation and selection for mediating effects of environmental change; and observation of community composition via metagenomic methods, to capture not just the bacterial component of the micro-ecosystems, but also to research the functional significance of other likely inhabitants, such as viruses. Finally, one could research why these micro-ecosystems did not become entirely oxic or entirely anoxic, and why there was little evidence of the discontinuous responses to environmental change that are predicted for systems with strong positive feedbacks, such as this one.

ACKNOWLEDGEMENTS

MS was funded by Forschungskredit of the UZH (FK-20-125). OLP was supported by the University of Zurich Research Priority Programs in Global Change and Biodiversity and the Swiss National Science Foundation (Project 310030_188431). We thank Robin Hostettler for technical support and Marcel Freund for preparing the light-gradient chambers. We thank the Functional Genomic Center Zurich for sequencing efforts and support with sequencing analysis.

CONFLICT OF INTEREST

None declared.

AUTHOR CONTRIBUTIONS

Marcel Suleiman: Conceptualization (lead); Data curation (lead); Funding acquisition (lead); Investigation (equal); Methodology (lead); Supervision (equal); Validation (equal); Visualization (equal); Writing-original draft (lead). **Yves Choffat:** Data curation (equal); Investigation (equal); Methodology (equal); Software (equal);

Writing-original draft (supporting); Writing-review & editing (supporting). **Uriah Daugaard:** Data curation (equal); Formal analysis (equal); Methodology (supporting); Validation (supporting); Visualization (equal); Writing-original draft (supporting); Writing-review & editing (supporting). **Owen Petchey:** Conceptualization (lead); Data curation (equal); Funding acquisition (lead); Investigation (equal); Methodology (equal); Resources (equal); Software (equal); Supervision (equal); Visualization (equal); Writing-original draft (lead); Writing-review & editing (lead).

ETHICS STATEMENT

None required.

DATA AVAILABILITY STATEMENT

Raw sequencing data are available at NCBI SRA under the BioSample accession numbers from SAMN16774060 to SAMN16774152; BioProject PRJNA677857: <https://www.ncbi.nlm.nih.gov/bioproject/PRJNA677857>

ORCID

Marcel Suleiman  <https://orcid.org/0000-0001-9141-8231>

REFERENCES

- Allison, S. D., Lu, Y., Weihe, C., Goulden, M. L., Martiny, A. C., Treseder, K. K., & Martiny, J. B. H. (2013). Microbial abundance and composition influence litter decomposition response to environmental change. *Ecology*, *94*, 714–725. <https://doi.org/10.1890/12-1243.1>
- Antranikian, G., Suleiman, M., Schäfers, C., Adams, M. W. W., Bartolucci, S., Blamey, J. M., Birkeland, N.-K., Bonch-Osmolovskaya, E., da Costa, M. S., Cowan, D., Danson, M., Forterre, P., Kelly, R., Ishino, Y., Littlechild, J., Moracci, M., Noll, K., Oshima, T., Robb, F., ... Stetter, K. O. (2017). Diversity of bacteria and archaea from two shallow marine hydrothermal vents from Vulcano Island. *Extremophiles*, *21*, 733–742. <https://doi.org/10.1007/s00792-017-0938-y>
- Balser, T. C., McMahon, K. D., Bart, D., Bronson, D., Coyle, D. R., Craig, N., Flores-Mangual, M. L., Forshay, K., Jones, S. E., Kent, A. E., & Shade, A. L. (2006). Bridging the gap between micro - and macro-scale perspectives on the role of microbial communities in global change ecology. *Plant and Soil*, *289*, 59–70. <https://doi.org/10.1007/s11104-006-9104-5>
- Beisner, B. E., & Cuddington, K. (2010). Alternative stable states in ecology. *Frontiers in Ecology and the Environment*, *327*, 259–266. <https://doi.org/10.1007/s10509-010-0328-8>
- Boetius, A. (2019). Global change microbiology – Big questions about small life for our future. *Nature Reviews Microbiology*, *17*, 331–332. <https://doi.org/10.1038/s41579-019-0197-2>
- Bush, T., Diao, M., Allen, R. J., Sinnige, R., Muyzer, G., & Huisman, J. (2017). Oxic-Anoxic regime shifts mediated by feedbacks between biogeochemical processes and microbial community dynamics. *Nature Communications*, *8*, 789. <https://doi.org/10.1038/s41467-017-00912-x>
- Callahan, B. J., McMurdie, P. J., Rosen, M. J., Han, A. W., Johnson, A. J. A., & Holmes, S. P. (2016). DADA2: High-resolution sample inference from Illumina amplicon data. *Nature Methods*, *13*, 581–583. <https://doi.org/10.1038/nmeth.3869>
- Cao, P., Lu, C., & Yu, Z. (2018). Historical nitrogen fertilizer use in agricultural ecosystems of the contiguous United States during 1850–2015: Application rate, timing, and fertilizer types. *Earth System Science Data*, *10*, 969–984. <https://doi.org/10.5194/essd-10-969-2018>

- Cavicchioli, R., Ripple, W. J., Timmis, K. N., Azam, F., Bakken, L. R., Baylis, M., Behrenfeld, M. J., Boetius, A., Boyd, P. W., Classen, A. T., Crowther, T. W., Danovaro, R., Foreman, C. M., Huisman, J., Hutchins, D. A., Jansson, J. K., Karl, D. M., Koskella, B., Mark Welch, D. B., ... Webster, N. S. (2019). Scientists' warning to humanity: Microorganisms and climate change. *Nature Reviews Microbiology*, 17, 569–586. <https://doi.org/10.1038/s41579-019-0222-5>
- Chapra, S. C., & Canale, R. P. (1991). Long-term phenomenological model of phosphorus and oxygen for stratified lakes. *Water Research*, 25, 707–715. [https://doi.org/10.1016/0043-1354\(91\)90046-5](https://doi.org/10.1016/0043-1354(91)90046-5)
- Cole, J. K., Peacock, J. P., Dodsworth, J. A., Williams, A. J., Thompson, D. B., Dong, H., Wu, G., & Hedlund, B. P. (2013). Sediment microbial communities in Great Hoiling Spring are controlled by temperature and distinct from water communities. *ISME Journal*, 7, 718–729. <https://doi.org/10.1038/ismej.2012.157>
- Coyle, D. R., Nagendra, U. J., Taylor, M. K., Campbell, J. H., Cunard, C. E., Joslin, A. H., Mundepe, A., Phillips, C. A., & Callahan, M. A. (2017). Soil fauna responses to natural disturbances, invasive species, and global climate change: Current state of the science and a call to action. *Soil Biology & Biochemistry*, 110, 116–133. <https://doi.org/10.1016/j.soilbio.2017.03.008>
- De Vos, M. G. J., Zagorski, M., McNally, A., & Bollenbach, T. (2017). Interaction networks, ecological stability, and collective antibiotic tolerance in polymicrobial infections. *Proceedings of the National Academy of Sciences USA*, 114, 10666–10671. <https://doi.org/10.1073/pnas.1713372114>
- Deng, Y. E., Ning, D., Qin, Y., Xue, K., Wu, L., He, Z., Yin, H., Liang, Y., Buzzard, V., Michaletz, S. T., & Zhou, J. (2018). Spatial scaling of forest soil microbial communities across a temperature gradient. *Environmental Microbiology*, 20, 3504–3513. <https://doi.org/10.1111/1462-2920.14303>
- Diao, M., Huisman, J., & Muyzer, G. (2018). Spatio-temporal dynamics of sulfur bacteria during oxic-anoxic regime shifts in a seasonally stratified lake. *FEMS Microbiology Ecology*, 94, fiy040. <https://doi.org/10.1093/femsec/fiy040>
- Diao, M., Sinnige, R., Kalbitz, K., Huisman, J., & Muyzer, G. (2017). Succession of bacterial communities in a seasonally stratified lake with an anoxic and sulfidic hypolimnion. *Frontiers in Microbiology*, 8, 2511. <https://doi.org/10.3389/fmicb.2017.02511>
- Dworkin, M., & Gutnick, D. (2012). Sergei Winogradsky: A founder of modern microbiology and the first microbial ecologist. *FEMS Microbiology Reviews*, 36, 364–379. <https://doi.org/10.1111/j.1574-6976.2011.00299.x>
- Dworkin, M., & Gutnick, D. (2012). Sergei Winogradsky: A founder of modern microbiology and the first microbial ecologist. *FEMS Microbiology Reviews*, 36, 364–379. <https://doi.org/10.1111/j.1574-6976.2011.00299.x>
- Evans, S. E., & Wallenstein, M. D. (2014). Climate change alters ecological strategies of soil bacteria. *Ecology Letters*, 17, 155–164. <https://doi.org/10.1111/ele.12206>
- Falkowski, P. G., Fenchel, T., & Delong, E. F. (2008). The microbial engines that drive earth's biogeochemical cycles. *Science*, 320, 1034–1039. <https://doi.org/10.1126/science.1153213>
- Findlay, A. J., & Kamyshny, A. (2017). Turnover rates of intermediate sulfur species (Sx2-, S0, S2O32-, S4O62-, SO32-) in anoxic freshwater and sediments. *Frontiers in Microbiology*, 8, 2551. <https://doi.org/10.3389/fmicb.2017.02551>
- Garcia, S. L., Salka, I., Grossart, H.-P., & Warnecke, F. (2013). Depth-discrete profiles of bacterial communities reveal pronounced spatio-temporal dynamics related to lake stratification. *Environmental Microbiology Reports*, 5, 549–555. <https://doi.org/10.1111/1758-2229.12044>
- Garcia-Pichel, F., Loza, V., Marusenko, Y., Mateo, P., & Potrafka, R. M. (2013). Temperature drives the continental-scale distribution of key microbes in topsoil communities. *Science*, 340, 1574–1577. <https://doi.org/10.1126/science.1236404>
- Gloor, G. B., Macklaim, J. M., Pawlowsky-Glahn, V., & Egozcue, J. J. (2017). Microbiome datasets are compositional: And this is not optional. *Frontiers in Microbiology*, 8, 2224. <https://doi.org/10.3389/fmicb.2017.02224>
- González-Varo, J. P., Biesmeijer, J. C., Bommarco, R., Potts, S. G., Schweiger, O., Smith, H. G., Steffan-Dewenter, I., Szentgyörgyi, H., Woyciechowski, M., & Vilà, M. (2013). Combined effects of global change pressures on animal-mediated pollination. *Trends in Ecology & Evolution*, 28, 524–530. <https://doi.org/10.1016/j.tree.2013.05.008>
- Gorham, E., & Boyce, F. M. (1989). Influence of lake surface area and depth upon thermal stratification and the depth of the summer thermocline. *Journal of Great Lakes Research*, 15, 233–245. [https://doi.org/10.1016/S0380-1330\(89\)71479-9](https://doi.org/10.1016/S0380-1330(89)71479-9)
- Guerrero, R., Montesinos, E., Pedrós-Alió, C., Esteve, I., Mas, J., van Gemerden, H., Hofman, P. A. G., & Bakker, J. F. (1985). Phototrophic sulfur bacteria in two Spanish lakes: Vertical distribution and limiting factors. *Limnology and Oceanography*, 30, 919–931. <https://doi.org/10.4319/lo.1985.30.5.0919>
- Guggenheim, C., Freimann, R., Mayr, M. J., Beck, K., Wehrli, B., & Bürgmann, H. (2020). Environmental and microbial interactions shape methane-oxidizing bacterial communities in a stratified lake. *Frontiers in Microbiology*, 11, 579427. <https://doi.org/10.3389/fmicb.2020.579427>
- Hamilton, T. L., Bovee, R. J., Thiel, V., Sattin, S. R., Mohr, W., Schaperdoth, I., Vogl, K., Gilhooly, W. P., Lyons, T. W., Tomsho, L. P., Schuster, S. C., Overmann, J., Bryant, D. A., Pearson, A., & Macalady, J. L. (2014). Coupled reductive and oxidative sulfur cycling in the phototrophic plate of a meromictic lake. *Geobiology*, 12, 451–468. <https://doi.org/10.1111/gbi.12092>
- Hutchins, D. A., & Fu, F. (2017). Microorganisms and ocean global change. *Nature Microbiology*, 2, 17058. <https://doi.org/10.1038/nmicrobiol.2017.58>
- Hutchins, D. A., Jansson, J. K., Remais, J. V., Rich, V. I., Singh, B. K., & Trivedi, P. (2019). Climate change microbiology – Problems and perspectives. *Nature Reviews Microbiology*, 17, 391–396. <https://doi.org/10.1038/s41579-019-0178-5>
- Jorgensen, B. B., Kuenen, J. G., & Cohen, Y. (1979). Microbial transformations of sulfur compounds in a stratified lake (Solar Lake, Sinai). *Limnology and Oceanography*, 24, 799–822. <https://doi.org/10.4319/lo.1979.24.5.0799>
- Kertesz, M. A. (2000). Riding the sulfur cycle – Metabolism of sulfonates and sulfate esters in Gram-negative bacteria. *FEMS Microbiology Reviews*, 24, 135–175. [https://doi.org/10.1016/S0168-6445\(99\)00033-9](https://doi.org/10.1016/S0168-6445(99)00033-9)
- Lahti, L., Salojärvi, J., Salonen, A., Scheffer, M., & de Vos, W. M. (2014). Tipping elements in the human intestinal ecosystem. *Nature Communications*, 5, 4344. <https://doi.org/10.1038/ncomms5344>
- Lee, J. Z., Burow, L. C., Woeckel, D., Everroad, R. C., Kubo, M. D., Spormann, A. M., Weber, P. K., Pett-Ridge, J., Bebout, B. M., & Hoehler, T. M. (2014). Fermentation couples Chloroflexi and sulfate-reducing bacteria to Cyanobacteria in hypersaline microbial mats. *Frontiers in Microbiology*, 5, 1–17. <https://doi.org/10.3389/fmicb.2014.00061>
- Luek, A., Rowan, D. J., & Rasmussen, J. B. (2017). N-P fertilization stimulates anaerobic selenium reduction in an end-pit lake. *Scientific Reports*, 7, 10502. <https://doi.org/10.1038/s41598-017-11095-2>
- Luther, G. W., Glazer, B., Ma, S., Trouwborst, R., Shultz, B. R., Druschel, G., & Kraiyya, C. (2003). Iron and sulfur chemistry in a stratified lake: Evidence for iron-rich sulfide complexes. *Aquatic Geochemistry*, 9, 87–110. <https://doi.org/10.1023/B:AQUA.0000019466.62564.94>
- McMurdie, P. J., & Holmes, S. (2013). Phyloseq: An R package for reproducible interactive analysis and graphics of microbiome census data. *PLoS One*, 8, e61217. <https://doi.org/10.1371/journal.pone.0061217>

- Morrison, J. M., Baker, K. D., Zamor, R. M., Nikolai, S., Elshahed, M. S., & Youssef, N. H. (2017). Spatiotemporal analysis of microbial community dynamics during seasonal stratification events in a freshwater lake (Grand Lake, OK, USA). *PLoS One*, *12*, 1–29. <https://doi.org/10.1371/journal.pone.0177488>
- Nedwell, D. B., Blackburn, T. H., & Wiebe, W. J. (1994). Dynamic nature of the turnover of organic carbon, nitrogen and sulphur in the sediments of a Jamaican mangrove forest. *Marine Ecology Progress Series*, *110*, 223–231.
- Niiranen, S., Yletyinen, J., Tomczak, M. T., Blenckner, T., Hjerne, O., MacKenzie, B. R., Müller-Karulis, B., Neumann, T., & Meier, H. E. M. (2013). Combined effects of global climate change and regional ecosystem drivers on an exploited marine food web. *Global Change Biology*, *19*, 3327–3342. <https://doi.org/10.1111/gcb.12309>
- Nyirabuhoro, P., Liu, M., Xiao, P., Liu, L., Yu, Z., Wang, L., & Yang, J. (2020). Seasonal variability of conditionally rare taxa in the water column bacterioplankton community of subtropical reservoirs in China. *Microbial Ecology*, *80*, 14–26. <https://doi.org/10.1007/s00248-019-01458-9>
- Oksanen, J., Blanchet, F. G., Friendly, M., Kindt, R., Legendre, P., Mcglinn, D., Minchin, P. R., O'hara, R. B., Simpson, G. L., Solymos, P., Henry, M., Stevens, H., Szoecs, E., & Maintainer, H. W. (2019). Package “vegan” title community ecology package. *Community Ecology Package*, *2*, 1–297.
- Overmann, J., & van Gernerden, H. (2000). Microbial interactions involving sulfur bacteria: Implications for the ecology and evolution of bacterial communities. *FEMS Microbiology Reviews*, *24*, 591–599. [https://doi.org/10.1016/S0168-6445\(00\)00047-4](https://doi.org/10.1016/S0168-6445(00)00047-4)
- Pagalina, E., Vassileva, K., Mills, C. G., Bush, T., Blythe, R. A., Schwarz-Linek, J., Strathdee, F., Allen, R. J., & Free, A. (2017). Assembly of microbial communities in replicate nutrient-cycling model ecosystems follows divergent trajectories, leading to alternate stable states. *Environmental Microbiology*, *19*, 3374–3386. <https://doi.org/10.1111/1462-2920.13849>
- Pennekamp, F., Pontarp, M., Tabi, A., Altermatt, F., Alther, R., Choffat, Y., Fronhofer, E. A., Ganesanandamoorthy, P., Garnier, A., Griffiths, J. I., Greene, S., Horgan, K., Massie, T. M., Mächler, E., Palamara, G. M., Seymour, M., & Petchey, O. L. (2018). Biodiversity increases and decreases ecosystem stability. *Nature*, *563*, 109–112. <https://doi.org/10.1038/s41586-018-0627-8>
- Pimenov, N. V., Zakharova, E. E., Bryukhanov, A. L., Korneeva, V. A., Kuznetsov, B. B., Tourova, T. P., Pogodaeva, T. V., Kalmychkov, G. V., & Zemskaya, T. I. (2014). Activity and structure of the sulfate-reducing bacterial community in the sediments of the southern part of Lake Baikal. *Microbiology*, *83*, 47–55. <https://doi.org/10.1134/S0026261714020167>
- Posch, T., Köster, O., Salcher, M. M., & Pernthaler, J. (2012). Harmful filamentous cyanobacteria favoured by reduced water turnover with lake warming. *Nature Climate Change*, *2*, 809–813. <https://doi.org/10.1038/nclimate1581>
- Procedure & Checklist - Amplification of Full-Length 16S Gene with Barcoded Primers for Multiplexed SMRTbell Library Preparation and Sequencing. 2020. <https://www.pacb.com/wp-content/uploads/Procedure-Checklist-%E2%80%93-Amplification-of-Full-Length-16S-Gene-with-Barcoded-Primers-for-Multiplexed-SMRTbell-Library-Preparation-and-Sequencing.pdf>
- Quast, C., Pruesse, E., Yilmaz, P., Gerken, J., Schweer, T., Yarza, P., Peplies, J., & Glöckner, F. O. (2012). The SILVA ribosomal RNA gene database project: Improved data processing and web-based tools. *Nucleic Acids Research*, *41*, D590–D596. <https://doi.org/10.1093/nar/gks1219>
- Rillig, M. C., Ryo, M., Lehmann, A., Aguilar-Trigueros, C. A., Buchert, S., Wulf, A., Iwasaki, A., Roy, J., & Yang, G. (2019). The role of multiple global change factors in driving soil functions and microbial biodiversity. *Science*, *366*, 886–890. <https://doi.org/10.1126/science.aay2832>
- Rundell, E. A., Banta, L. M., Ward, D. V., Watts, C. D., Birren, B., & Esteban, D. J. (2014). 16S rRNA gene survey of microbial communities in Winogradsky columns. *PLoS One*, *9*, e104134. <https://doi.org/10.1371/journal.pone.0104134>
- Sass, H., Cypionka, H., & Babenzien, H.-D. (1997). Vertical distribution of sulfate-reducing bacteria at the oxic-anoxic interface in sediments of the oligotrophic Lake Stechlin. *FEMS Microbiology Ecology*, *22*, 245–255. <https://doi.org/10.1111/j.1574-6941.1997.tb00377.x>
- Savvichev, A. S., Babenko, V. V., Lunina, O. N., Letarova, M. A., Boldyreva, D. I., Veslopolova, E. F., Demidenko, N. A., Kokryatskaya, N. M., Krasnova, E. D., Gaisin, V. A., Kostryukova, E. S., Gorlenko, V. M., & Letarov, A. V. (2018). Sharp water column stratification with an extremely dense microbial population in a small meromictic lake, Trekhtzvetnoe. *Environmental Microbiology*, *20*, 3784–3797. <https://doi.org/10.1111/1462-2920.14384>
- Schulte to Bühne, H., Tobias, J. A., Durant, S. M., & Petteorelli, N. (2020). Improving predictions of climate change-land use change interactions. *Trends in Ecology & Evolution*, *36*, 29–38. <https://doi.org/10.1016/j.tree.2020.08.019>
- Stein, L. Y., & Klotz, M. G. (2016). The nitrogen cycle. *Current Biology*, *26*, R94–R98. <https://doi.org/10.1016/j.cub.2015.12.021>
- Suleiman, M., Klippel, B., Busch, P., Schäfers, C., Moccand, C., Bel-Rhliid, R., Palzer, S., & Antranikian, G. (2019). Enrichment of anaerobic heterotrophic thermophiles from four Azorean hot springs revealed different community composition and genera abundances using recalcitrant substrates. *Extremophiles*, *23*, 277–281. <https://doi.org/10.1007/s00792-019-01079-7>
- Tylianakis, J. M., Didham, R. K., Bascompte, J., & Wardle, D. A. (2008). Global change and species interactions in terrestrial ecosystems. *Ecology Letters*, *11*, 1351–1363. <https://doi.org/10.1111/j.1461-0248.2008.01250.x>
- Vavourakis, C. D., Mehrshad, M., Balkema, C., van Hall, R., Andrei, A.-Ş., Ghai, R., Sorokin, D. Y., & Muyzer, G. (2019). Metagenomes and metatranscriptomes shed new light on the microbial-mediated sulfur cycle in a Siberian soda lake. *BMC Biology*, *17*, 1–20. <https://doi.org/10.1186/s12915-019-0688-7>
- Velthuis, M., Kosten, S., Aben, R., Kazanjian, G., Hilt, S., Peeters, E. T. H. M., Donk, E., & Bakker, E. S. (2018). Warming enhances sedimentation and decomposition of organic carbon in shallow macrophyte-dominated systems with zero net effect on carbon burial. *Global Change Biology*, *24*, 5231–5242. <https://doi.org/10.1111/gcb.14387>
- Vigneron, A., Cruaud, P., Culley, A. I., Couture, R.-M., Lovejoy, C., & Vincent, W. F. (2021). Genomic evidence for sulfur intermediates as new biogeochemical hubs in a model aquatic microbial ecosystem. *Microbiome*, *9*, 46. <https://doi.org/10.1186/s40168-021-00999-x>
- Weiss, J. V., Emerson, D., Backer, S. M., & Megonigal, J. P. (2003). Enumeration of Fe(II)-oxidizing and Fe(III)-reducing bacteria in the root zone of wetland plants: Implications for a rhizosphere iron cycle. *Biogeochemistry*, *64*, 77–96. <https://doi.org/10.1023/A:1024953027726>
- Widder, S., Allen, R. J., Pfeiffer, T., Curtis, T. P., Wiuf, C., Sloan, W. T., Cordero, O. X., Brown, S. P., Momeni, B., Shou, W., Kettle, H., Flint, H. J., Haas, A. F., Laroche, B., Kreft, J.-U., Rainey, P. B., Freilich, S., Schuster, S., Milferstedt, K., ... Soyer, O. S. (2016). Challenges in microbial ecology: Building predictive understanding of community function and dynamics. *ISME Journal*, *10*, 2557–2568. <https://doi.org/10.1038/ismej.2016.45>
- Wörner, S., & Pester, M. (2019). The active sulfate-reducing microbial community in littoral sediment of oligotrophic Lake Constance. *Frontiers in Microbiology*, *10*, 247. <https://doi.org/10.3389/fmicb.2019.00247>

- Wu, K., Zhao, W., Wang, Q., Yang, X., Zhu, L., Shen, J. I., Cheng, X., & Wang, J. (2019). The relative abundance of benthic bacterial phyla along a water-depth gradient in a plateau lake: Physical, chemical, and biotic drivers. *Frontiers in Microbiology*, 10, 1521. <https://doi.org/10.3389/fmicb.2019.01521>
- Yu, Z., Yang, J., Amalfitano, S., Yu, X., & Liu, L. (2014). Effects of water stratification and mixing on microbial community structure in a subtropical deep reservoir. *Scientific Reports*, 4, 1–7. <https://doi.org/10.1038/srep05821>
- Zavarzin, G. A. (2006). Winogradsky and modern microbiology. *Microbiology*, 75, 501–511. <https://doi.org/10.1134/S0026261706050018>

How to cite this article: Suleiman M, Choffat Y, Daugaard U, Petchey OL. Large and interacting effects of temperature and nutrient addition on stratified microbial ecosystems in a small, replicated, and liquid-dominated Winogradsky column approach. *MicrobiologyOpen*. 2021;10:e1189. <https://doi.org/10.1002/mbo3.1189>

APPENDIX

TABLE A1 Overview of filtered reads using DADA2 (Callahan et al., 2016)

Barcode	Sample_name	ccs	primers	filtered	denoised
lima.bc1005--bc1033.fastq.gz	Control_1_12_top	11208	9101	6763	4622
lima.bc1005--bc1035.fastq.gz	Control_1_12_bottom	14697	12225	9389	7023
lima.bc1005--bc1044.fastq.gz	Control_1_12_soil	10932	9265	6696	2789
lima.bc1005--bc1045.fastq.gz	Control_2_12_liquid	15954	13307	10179	7598
lima.bc1005--bc1054.fastq.gz	Control_2_12_soil	10105	8619	5995	2091
lima.bc1005--bc1056.fastq.gz	Control_3_12_liquid	13063	10992	8283	4955
lima.bc1005--bc1057.fastq.gz	Control_3_12_soil	11150	9513	6792	2537
lima.bc1005--bc1059.fastq.gz	Fertilizer_1_12_top	21313	17187	12274	7803
lima.bc1005--bc1060.fastq.gz	Fertilizer_1_12_bottom	26033	20668	16280	12525
lima.bc1005--bc1062.fastq.gz	Fertilizer_1_12_soil	12366	10480	7946	3950
lima.bc1005--bc1065.fastq.gz	Fertilizer_2_12_liquid	22018	17748	13626	9962
lima.bc1005--bc1075.fastq.gz	Fertilizer_2_12_soil	17161	14369	10597	5298
lima.bc1007--bc1033.fastq.gz	Fertilizer_3_12_liquid	17291	14072	10408	7178
lima.bc1007--bc1035.fastq.gz	Fertilizer_3_12_soil	12363	10326	7844	3978
lima.bc1007--bc1044.fastq.gz	Control_1_16_top	12097	10430	8602	7368
lima.bc1007--bc1045.fastq.gz	Control_1_16_bottom	27061	22460	16889	12418
lima.bc1007--bc1056.fastq.gz	Control_2_16_liquid	15572	13054	10350	8131
lima.bc1007--bc1057.fastq.gz	Control_3_16_liquid	15383	13123	10570	8137
lima.bc1007--bc1059.fastq.gz	Control_3_16_soil	13905	11885	9188	4404
lima.bc1007--bc1060.fastq.gz	Fertilizer_1_16_top	19101	15896	12734	10395
lima.bc1007--bc1062.fastq.gz	Fertilizer_1_16_bottom	15544	12838	9626	6960
lima.bc1007--bc1065.fastq.gz	Fertilizer_1_16_soil	11824	10203	7648	3157
lima.bc1007--bc1075.fastq.gz	Fertilizer_2_16_liquid	15915	13385	10230	7476
lima.bc1008--bc1033.fastq.gz	Fertilizer_2_16_soil	13872	11851	8438	3610
lima.bc1008--bc1035.fastq.gz	Fertilizer_3_16_liquid	16244	13253	10213	7329
lima.bc1008--bc1044.fastq.gz	Fertilizer_3_16_soil	12733	10844	8183	3411
lima.bc1008--bc1045.fastq.gz	Control_1_20_top	16107	13825	11156	9366
lima.bc1008--bc1054.fastq.gz	Control_1_20_bottom	11308	9295	5916	2672
lima.bc1008--bc1056.fastq.gz	Control_1_20_soil	12476	10701	7939	3197
lima.bc1008--bc1057.fastq.gz	Control_2_20_liquid	9956	8298	5411	2047
lima.bc1008--bc1059.fastq.gz	Control_2_20_soil	11406	9750	6871	2594
lima.bc1008--bc1060.fastq.gz	Control_3_20_liquid	15686	12992	9432	6293
lima.bc1008--bc1062.fastq.gz	Control_3_20_soil	12175	10393	7722	3366
lima.bc1008--bc1065.fastq.gz	Fertilizer_1_20_top	16669	14407	11244	9289

(Continues)

TABLE A1 (Continued)

Barcode	Sample_name	ccs	primers	filtered	denoised
lima.bc1008--bc1075.fastq.gz	Fertilizer_1_20_bottom	13795	11067	7379	4067
lima.bc1012--bc1033.fastq.gz	Fertilizer_1_20_soil	11744	9974	6867	2764
lima.bc1012--bc1035.fastq.gz	Fertilizer_2_20_liquid	15010	12079	8970	6112
lima.bc1012--bc1044.fastq.gz	Fertilizer_2_20_soil	11767	9950	7077	3031
lima.bc1012--bc1045.fastq.gz	Fertilizer_3_20_liquid	15002	12425	8727	5558
lima.bc1012--bc1054.fastq.gz	Fertilizer_3_20_soil	12941	11130	7908	3307
lima.bc1012--bc1056.fastq.gz	Control_1_24_top	18781	15805	11961	9179
lima.bc1012--bc1057.fastq.gz	Control_1_24_bottom	21152	17404	13310	9656
lima.bc1012--bc1059.fastq.gz	Control_1_24_soil	13012	11267	8381	3693
lima.bc1012--bc1060.fastq.gz	Control_2_24_liquid	17029	14136	10004	6279
lima.bc1012--bc1062.fastq.gz	Control_2_24_soil	11978	10383	7455	3115
lima.bc1012--bc1065.fastq.gz	Control_3_24_liquid	15613	12868	8919	5255
lima.bc1012--bc1075.fastq.gz	Control_3_24_soil	10544	9186	6738	2740
lima.bc1015--bc1033.fastq.gz	Fertilizer_1_24_top	18728	15445	11359	8057
lima.bc1015--bc1035.fastq.gz	Fertilizer_1_24_bottom	24147	18452	13144	9133
lima.bc1015--bc1044.fastq.gz	Fertilizer_1_24_soil	14935	12243	9102	4679
lima.bc1015--bc1045.fastq.gz	Fertilizer_2_24_liquid	29251	22869	18567	14859
lima.bc1015--bc1054.fastq.gz	Fertilizer_2_24_soil	15617	13004	9814	5225
lima.bc1015--bc1056.fastq.gz	Fertilizer_3_24_liquid	21563	17051	13168	9750
lima.bc1015--bc1057.fastq.gz	Fertilizer_3_24_soil	13373	11238	7959	3369
lima.bc1015--bc1059.fastq.gz	Control_1_28_top	19970	16694	13642	11694
lima.bc1015--bc1060.fastq.gz	Control_1_28_bottom	37364	27999	22301	17159
lima.bc1015--bc1062.fastq.gz	Control_1_28_soil	13786	11618	8484	3807
lima.bc1015--bc1065.fastq.gz	Control_2_28_liquid	39234	29780	24880	19990
lima.bc1015--bc1075.fastq.gz	Control_2_28_soil	18126	14750	11344	6498
lima.bc1020--bc1033.fastq.gz	Control_3_28_liquid	19649	15721	11105	7004
lima.bc1020--bc1035.fastq.gz	Control_3_28_soil	11755	9977	6906	2516
lima.bc1020--bc1044.fastq.gz	Fertilizer_1_28_top	15550	12677	8602	5347
lima.bc1020--bc1045.fastq.gz	Fertilizer_1_28_bottom	25320	19704	15039	11223
lima.bc1020--bc1054.fastq.gz	Fertilizer_1_28_soil	14418	12217	8984	4639
lima.bc1020--bc1056.fastq.gz	Fertilizer_2_28_liquid	24646	19738	12250	8726
lima.bc1020--bc1057.fastq.gz	Fertilizer_2_28_soil	14416	12193	8881	4105
lima.bc1020--bc1059.fastq.gz	Fertilizer_3_28_liquid	26606	20726	15288	11249
lima.bc1020--bc1060.fastq.gz	Fertilizer_3_28_soil	15781	13476	9889	4587
lima.bc1020--bc1062.fastq.gz	Control_1_32_top	17079	14006	9512	6366
lima.bc1020--bc1065.fastq.gz	Control_1_32_bottom	38835	29503	24751	19178
lima.bc1020--bc1075.fastq.gz	Control_1_32_soil	16390	13178	9787	5511
lima.bc1022--bc1033.fastq.gz	Control_2_32_liquid	17994	13976	10740	7659
lima.bc1022--bc1035.fastq.gz	Control_2_32_soil	20127	16370	12945	8261
lima.bc1022--bc1044.fastq.gz	Control_3_32_liquid	38738	29140	24269	19389
lima.bc1022--bc1045.fastq.gz	Control_3_32_soil	22462	18325	14629	9593
lima.bc1022--bc1054.fastq.gz	Fertilizer_1_32_top	23460	18649	13503	9477
lima.bc1022--bc1056.fastq.gz	Fertilizer_1_32_bottom	31962	24799	20393	16009
lima.bc1022--bc1057.fastq.gz	Fertilizer_1_32_soil	15712	13224	10305	5926
lima.bc1022--bc1059.fastq.gz	Fertilizer_2_32_liquid	21375	16959	11827	8030

(Continues)

TABLE A1 (Continued)

Barcode	Sample_name	ccs	primers	filtered	denoised
lima.bc1022--bc1060.fastq.gz	Fertilizer_2_32_soil	16752	13991	10042	5099
lima.bc1022--bc1062.fastq.gz	Fertilizer_3_32_liquid	18579	14928	10576	7118
lima.bc1022--bc1065.fastq.gz	Fertilizer_3_32_soil	15963	13436	9729	4798
lima.bc1022--bc1075.fastq.gz	Control_1_36_top	18406	15017	9492	6871
lima.bc1024--bc1033.fastq.gz	Control_1_36_bottom	18247	14874	11026	7971
lima.bc1024--bc1035.fastq.gz	Control_1_36_soil	12527	10460	7696	4211
lima.bc1024--bc1044.fastq.gz	Control_2_36_liquid	20876	16714	12481	8982
lima.bc1024--bc1045.fastq.gz	Control_3_36_liquid	20002	16421	11207	7524
lima.bc1024--bc1054.fastq.gz	Control_3_36_soil	18348	15465	11839	7923
lima.bc1024--bc1056.fastq.gz	Fertilizer_1_36_top	51021	39246	18709	15036
lima.bc1024--bc1057.fastq.gz	Fertilizer_1_36_bottom	50990	40406	24346	19012
lima.bc1024--bc1059.fastq.gz	Fertilizer_1_36_soil	30440	25570	16925	9677
lima.bc1024--bc1060.fastq.gz	Fertilizer_2_36_liquid	39541	31773	19011	12428
lima.bc1024--bc1062.fastq.gz	Fertilizer_2_36_soil	20914	17751	12439	6742
lima.bc1024--bc1065.fastq.gz	Fertilizer_3_36_liquid	15419	12470	7084	3717
lima.bc1024--bc1075.fastq.gz	Fertilizer_3_36_soil	16104	13526	9769	5597

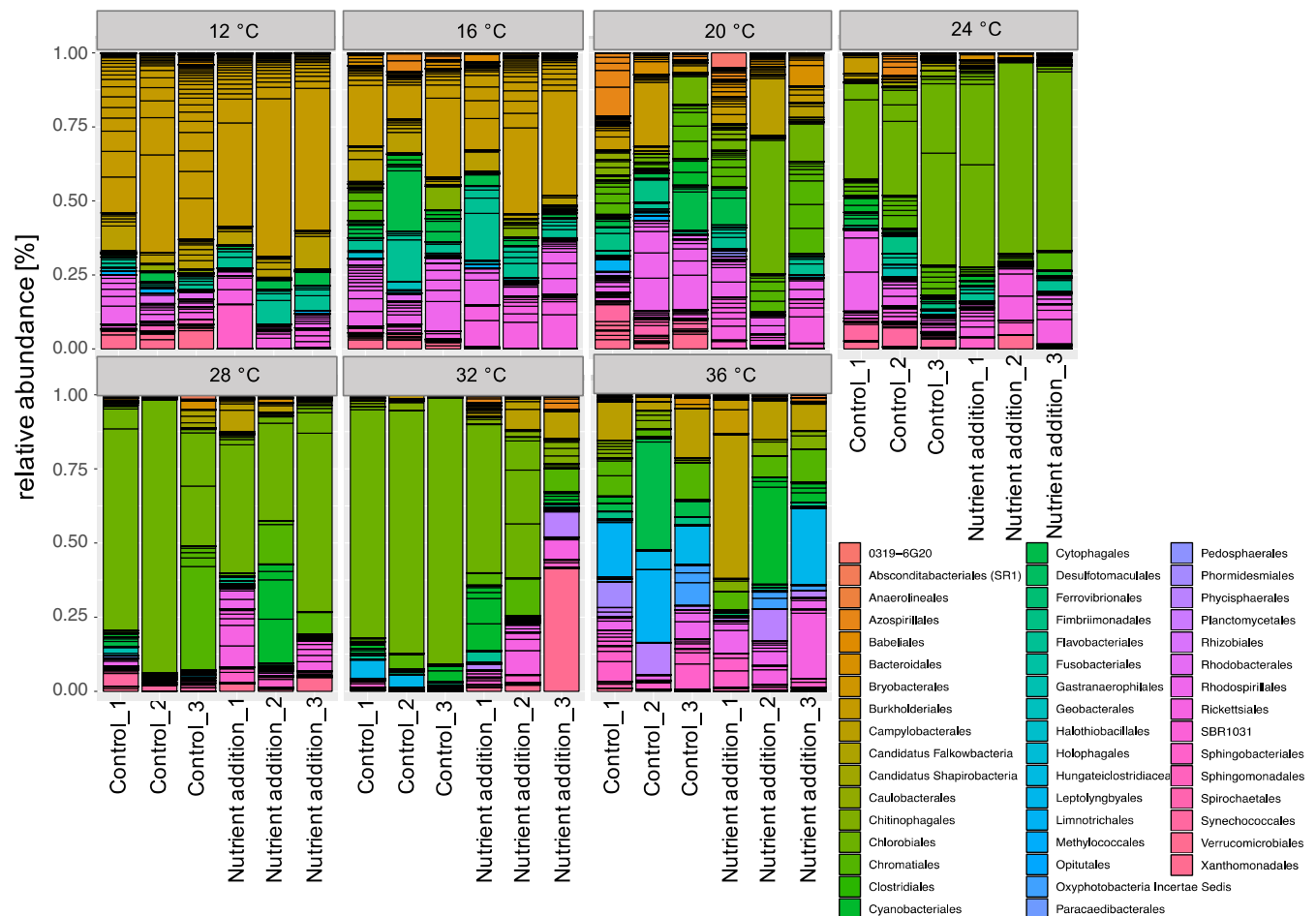


FIGURE A1 Microbial community composition of the liquid part of all micro-ecosystems. Relative abundance on order level is shown for each micro-ecosystem

FIGURE A2 Microbial community composition of the liquid part of the micro-ecosystems incubated at 12°C. Relative abundance on the genus level is shown for each micro-ecosystem. Relative abundances of specific genera <3% were assigned to "other"

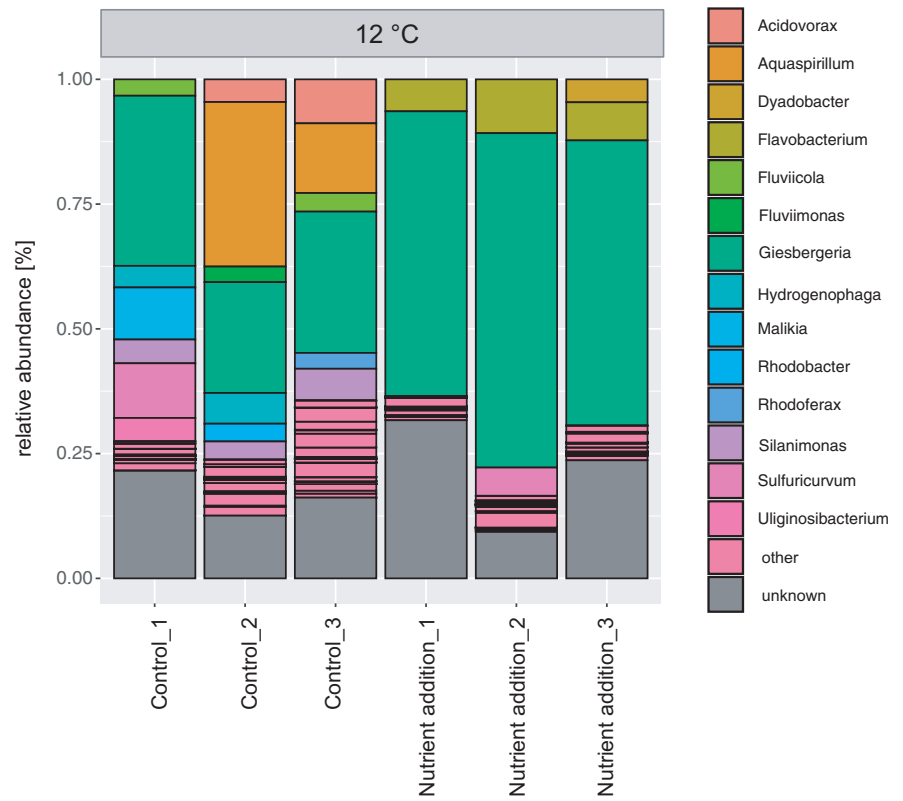
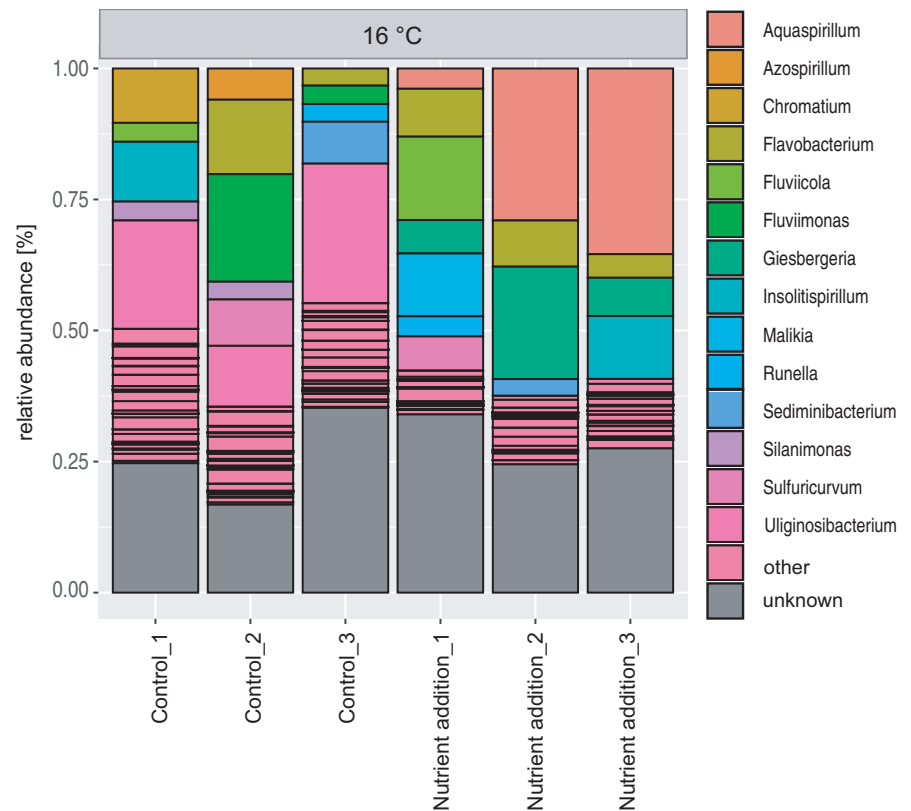


FIGURE A3 Microbial community composition of the liquid part of the micro-ecosystems incubated at 16°C. Relative abundance on the genus level is shown for each micro-ecosystem. Relative abundances of specific genera <3% were assigned to "other"



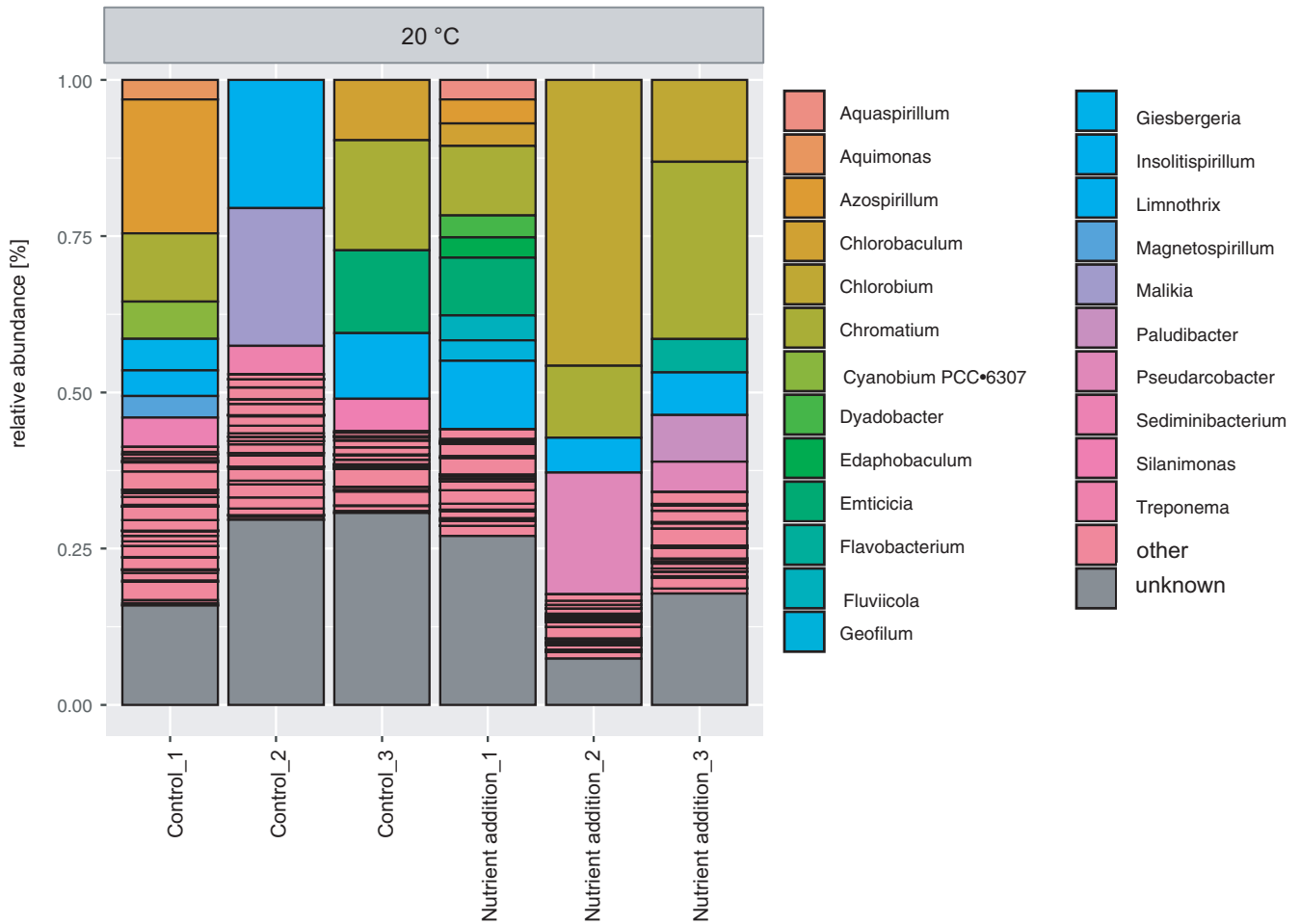


FIGURE A4 Microbial community composition of the liquid part of the micro-ecosystems incubated at 20°C. Relative abundance on the genus level is shown for each micro-ecosystem. Relative abundances of specific genera <3% were assigned to “other”

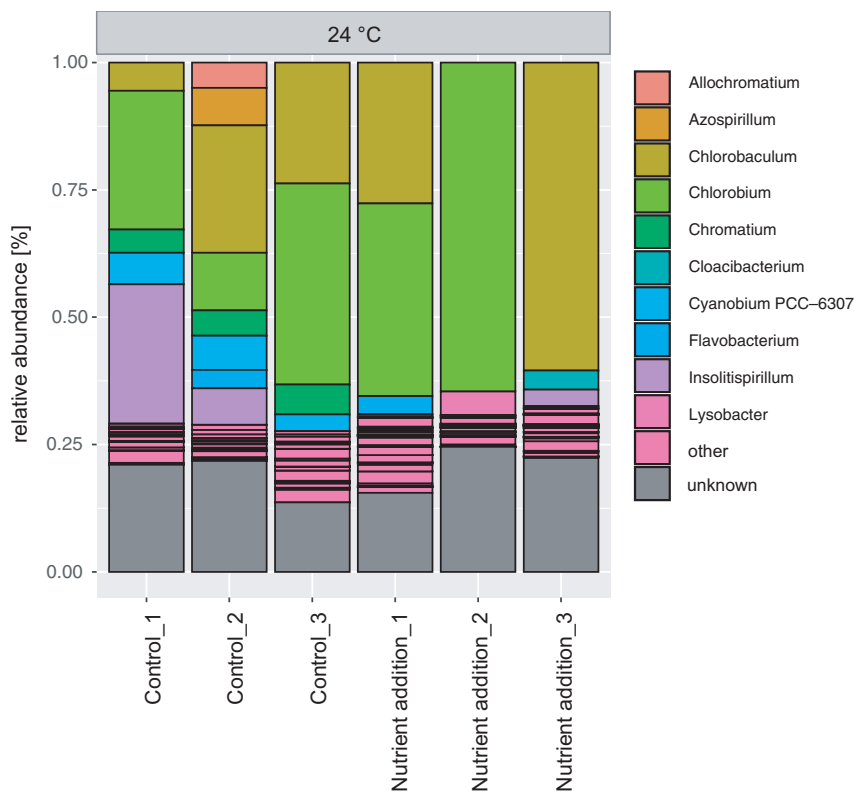


FIGURE A5 Microbial community composition of the liquid part of the micro-ecosystems incubated at 24°C. Relative abundance on the genus level is shown for each micro-ecosystem. Relative abundances of specific genera <3% were assigned to “other”

FIGURE A6 Microbial community composition of the liquid part of the micro-ecosystems incubated at 28°C. Relative abundance on the genus level is shown for each micro-ecosystem. Relative abundances of specific genera <3% were assigned to "other"

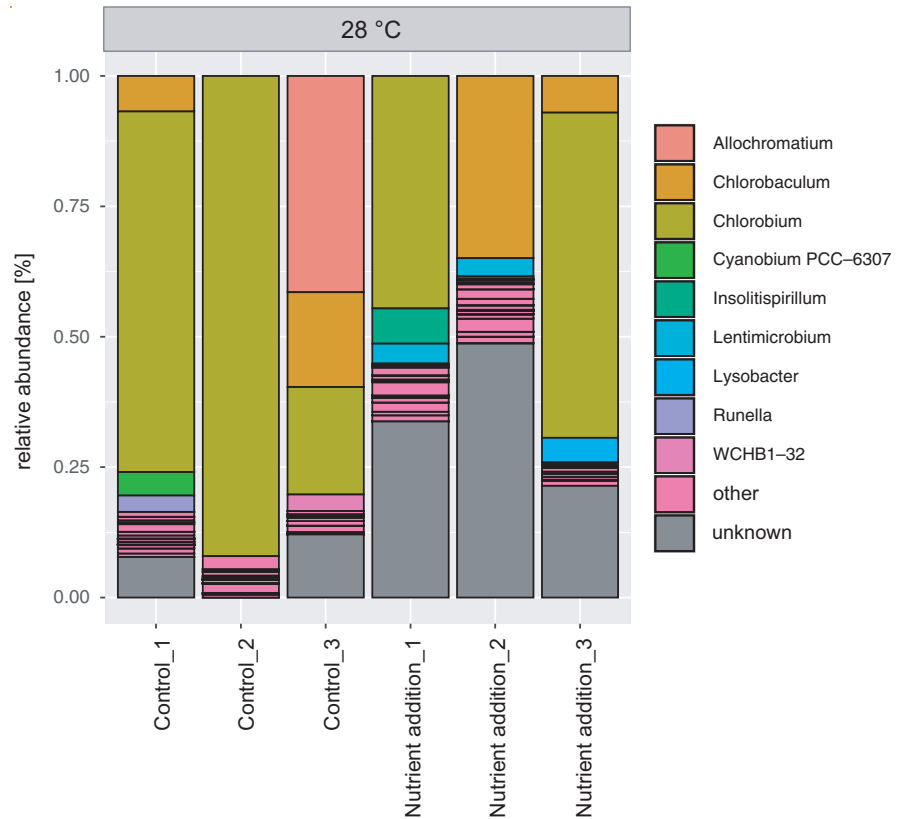
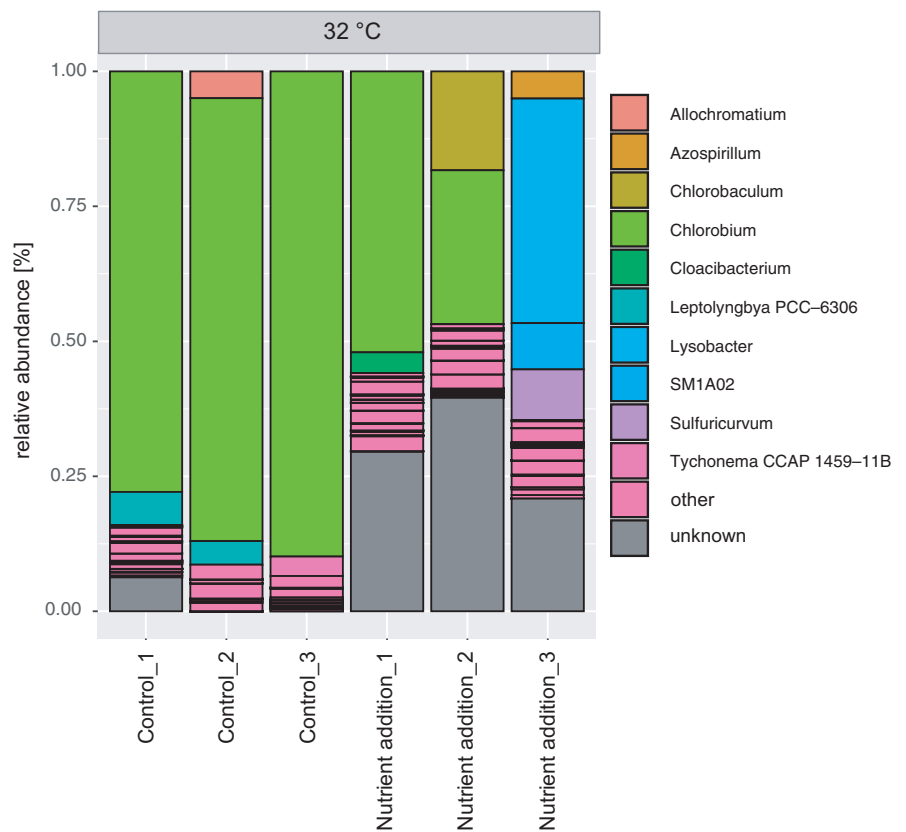


FIGURE A7 Microbial community composition of the liquid part of the micro-ecosystems incubated at 32°C. Relative abundance on the genus level is shown for each micro-ecosystem. Relative abundances of specific genera <3% were assigned to "other"



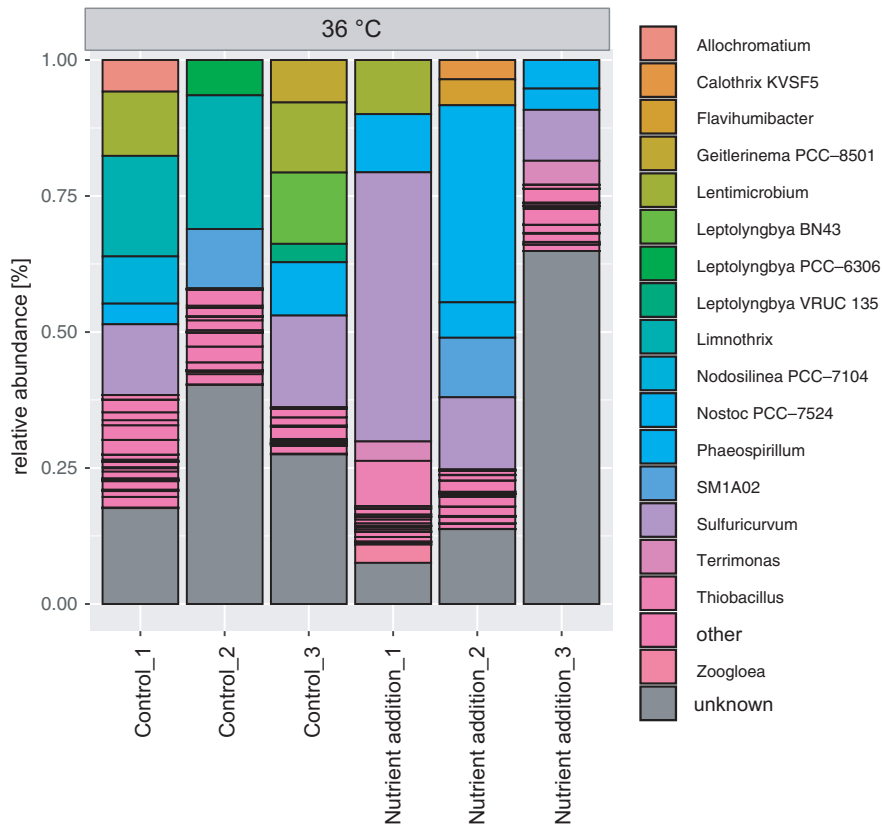


FIGURE A8 Microbial community composition of the liquid part of the micro-ecosystems incubated at 36°C. Relative abundance on the genus level is shown for each micro-ecosystem. Relative abundances of specific genera <3% were assigned to "other"

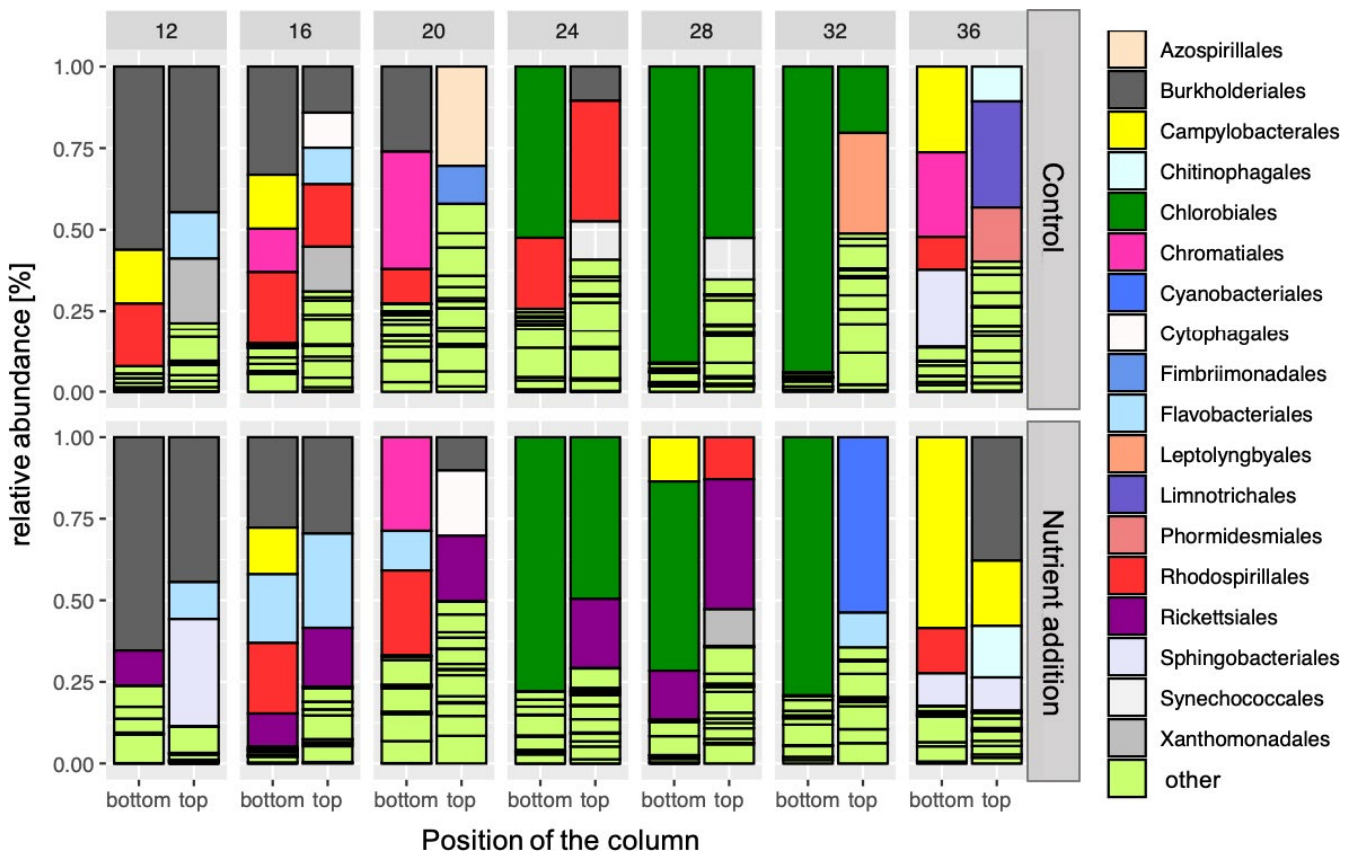


FIGURE A9 Microbial community composition of the upper and lower liquid part of replicate 1 of all treatments. The liquid part was separated at height of the bottom oxygen layer and both layers were sequenced separately. Relative abundances of specific orders <10% were assigned to "other"

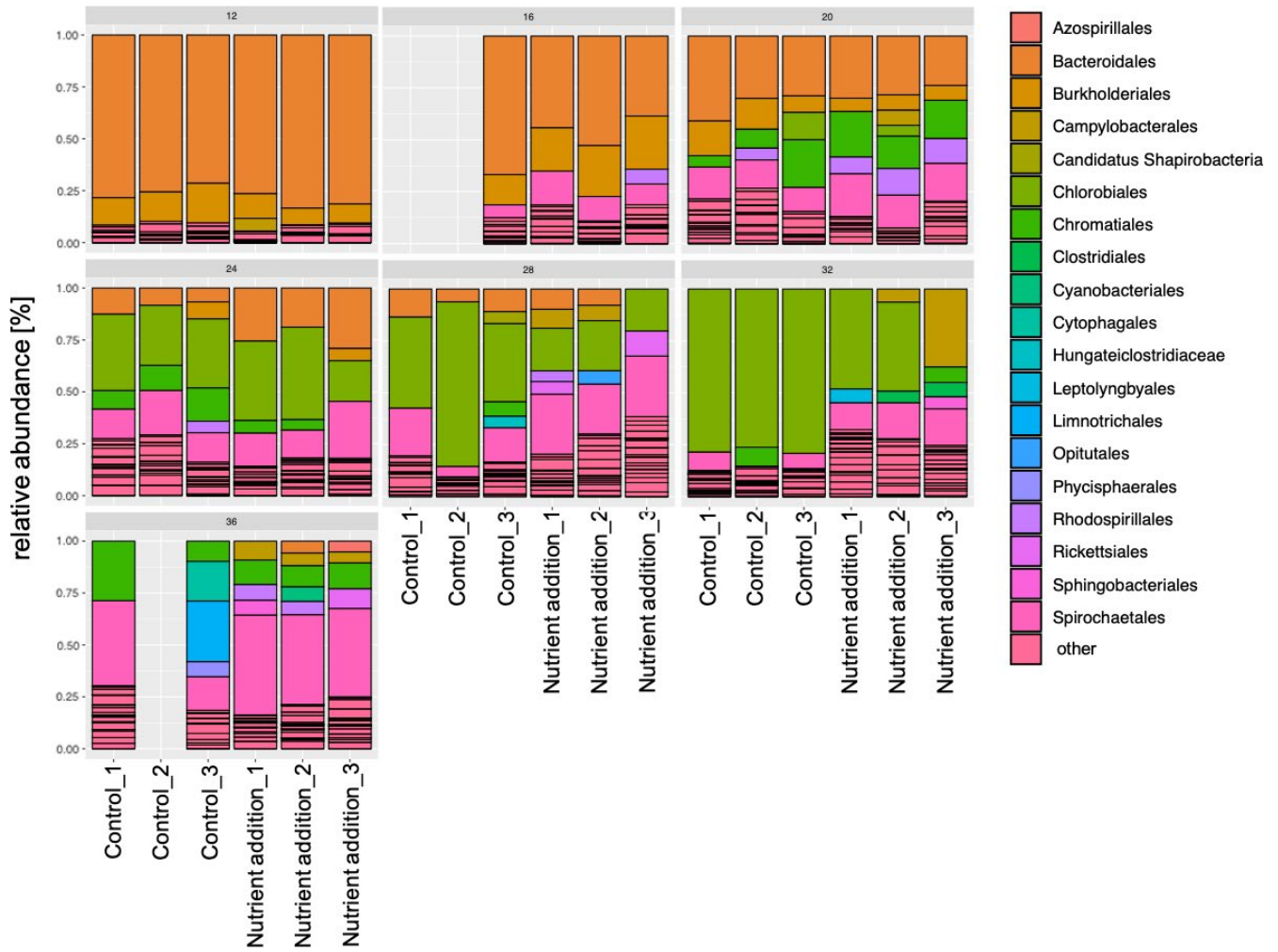


FIGURE A10 Microbial community composition of the sediments of the micro-ecosystems. Relative abundance on order level is shown for each micro-ecosystem. Three sequencing reactions were not successful. Relative abundances of specific order <10% were assigned to "other"